Structure and Reactivity of η^2(3e)-Nitrile and η^2(3e)-Alkyne Complexes of Niobium

Michel Etienne,*,† Carla Carfagna, Philippe Lorente, René Mathieu, and Dominique de Montauzon

Laboratoire de Chimie de Coordination du CNRS, UPR 8241, 205 Route de Narbonne, 31077 Toulouse Cedex 4, France

Received February 22, 1999

Nitrile adducts of the type Tp*Nb(CO)(PhC≡CMe)(RC≡N) (Tp* = hydridotris(3,5-dimethylpyrazolyl)borate; R = Me (**2a**), Et (**2b**), $PhCH_2$ (**2c**), 4-$MeOC_6H_5$ (**2d**), Ph (**2e**), 4-$CF_3C_6H_5$ (**2f**)) have been prepared in fair yields by CO displacement from Tp*Nb$(CO)_2$(PhC≡CMe) (**1**) and fully characterized. ^{13}C NMR spectroscopy (δ 180−190 for the nitrile and alkyne contact carbons) and X-ray crystallography (for **2b**) indicate an η^2-coordination and an unprecedented formally three-electron-donor (3e) behavior for both the alkyne and the nitrile. Electrochemical studies suggest that an equilibrium between this η^2(3e)-nitrile/η^2(3e)-alkyne form and an otherwise undetected η^1(2e)-nitrile/η^2(4e)-alkyne form exists in solution. PhC≡N is thermally displaced from **2e** by PMe_2Ph or PhC≡CMe to give Tp*Nb(CO)(PhC≡CMe)(PMe_2Ph) or Tp*Nb(CO)(PhC≡CMe)$_2$ (**3a**), respectively. **3a** does not react with PMe_2Ph. Protonation of **2b** with HBF_4 induces nitrile/alkyne coupling to give the niobacycle Tp*NbF(CPhCMeCPhNH), via the isolated η^2-iminoacyl alkyne cation [Tp*Nb(CO)(η^2-CPh═NH)(PhC≡CMe)][BF_4], characterized by NMR spectroscopy at 243 K. Protonation of **3a** with HBF_4 leads to the niobacycle Tp*NbF[C(Ph)C(Me)C(CMe═CPhH)O] (X-ray structure), in which CO is included in the alkyne coupling reaction. The intermediate [Tp*Nb(CO)(CMe═CPhH)(PhC≡CMe)][BF_4] has been characterized by NMR at 193 K. A deshielded C_α (δ 205), a shielded C_β (δ 97), and a reduced $^1J_{CH}$ (114 Hz) suggest that a β-CH agostic interaction stabilizes this vinyl alkyne cation. Protonation of the new phosphinoalkyne derivative Tp*Nb(CO)(PhC≡CMe)(PPh_2C≡CPh) affords the stable phosphonium complex {Tp*Nb(CO)[Ph_2P(H)C≡CPh](PhC≡CMe)}[BF_4], in which the two alkyne ligands act as 3e donors.

Introduction

Nitriles most often coordinate to single transition-metal centers in an η^1-fashion, behaving as weak σ-donors and π-acceptors.[1] In few instances, the nitrile is η^2-bound, and the lone pair on the nitrogen atom is not involved in the coordination. The nitrile then acts as a two-electron (2e), σ-donor/π-acceptor ligand via, respectively, the occupied $\pi_{||}$ and vacant $\pi^*_{||}$ orbitals of the carbon−nitrogen triple bond (|| refers to the plane of coordination). The complexes must then be regarded as electronically saturated.[2] Whereas the participation of the second π-system of alkynes, namely $\pi_\perp$, has been known for years,[3] the recognition that nitriles could behave similarly is very recent.[4] Harman,[4a,b] Richmond,[5] Young[6] and their co-workers have been involved in the area. In addition to the $\pi_{||}/\pi^*_{||}$ framework as observed for η^2(2e)-coordination, interaction of the occupied $\pi_\perp$ with a suitable empty metal d orbital allows the nitrile to act as a π-base, thus lending the basis for an η^2(4e) description of the bonding.[4−6] Wherever such a metal-based orbital was unavailable, notably for symmetry reasons, then the nitrile would formally donate less than four, yet more than two, electrons. In a preliminary communication, we described such a situation where two potentially 4e ligands, namely an alkyne and a nitrile, could only provide six electrons as a whole to a niobium(I) atom, thus formally behaving as 3e donors.[7] This represents a unique example of a 3e nitrile and nicely fills the gap between known η^2(2e)- and η^2(4e)-nitrile behaviors. A parallel situation is well-established for alkynes.[3]

† E-mail: etienne@lcc-toulouse.fr.

(1) Storhoff, B. N.; Lewis, H. C. *Coord. Chem. Rev.* **1977**, *23*, 1.
(2) (a) Thomas, J. L. *J. Am. Chem. Soc.* **1975**, *97*, 5943. (b) Bullock, R. M.; Headford, C. E. L.; Kegley, S. E.; Norton, J. R. *J. Am. Chem. Soc.* **1985**, *107*, 727. (c) Wright, T. C.; Wilkinson, G.; Motevalli, M.; Hursthouse, M. B. *J. Chem. Soc., Dalton Trans.* **1986**, 2017. (d) Chetcuti, P. A.; Knobler, C. B.; Hawthorne, M. F. *Organometallics* **1988**, *7*, 650. (e) Green, M. L. H.; Hughes, A. K.; Mountford, P. *J. Chem. Soc., Dalton Trans.* **1991**, 1407. (f) Lucas, D.; Modarres-Tehrani, Z.; Mugnier, Y.; Antinolo, A.; del Hierrio, I.; Fajardo, M. *New J. Chem.* **1996**, *20*, 385.
(3) Templeton, J. L. *Adv. Organomet. Chem.* **1989**, *29*, 1.
(4) (a) Barrera, J.; Sabat, M.; Harman, W. D. *Organometallics* **1993**, *12*, 4381. (b) Barrera, J.; Sabat, M.; Harman, W. D. *J. Am. Chem. Soc.* **1991**, *113*, 8178. (c) Anderson, S. J.; Wells, F. J.; Wilkinson, G.; Hussain, B.; Hursthouse, M. B. *Polyhedron* **1988**, *7*, 2615.
(5) (a) Kiplinger, J. L.; Arif, A. M.; Richmond, T. G. *Organometallics* **1997**, *16*, 246. (b) Kiplinger, J. L.; Arif, A. M.; Richmond, T. G. *Chem. Commun.* **1996**, 1691.
(6) (a) Thomas, S.; Young, C. G.; Tiekink, E. R. T. *Organometallics* **1998**, *17*, 182. (b) Thomas, S.; Lim, P. J.; Gable, R. W.; Young, C. G. *Inorg. Chem.* **1998**, *37*, 590. (c) Thomas, S.; Tiekink, E. R. T.; Young, C. G. *Organometallics* **1996**, *15*, 2428.
(7) Lorente, P.; Carfagna, C.; Etienne, M.; Donnadieu, B. *Organometallics* **1996**, *15*, 1090.

10.1021/om990119k CCC: $18.00
Publication on Web 07/08/1999

Scheme 1

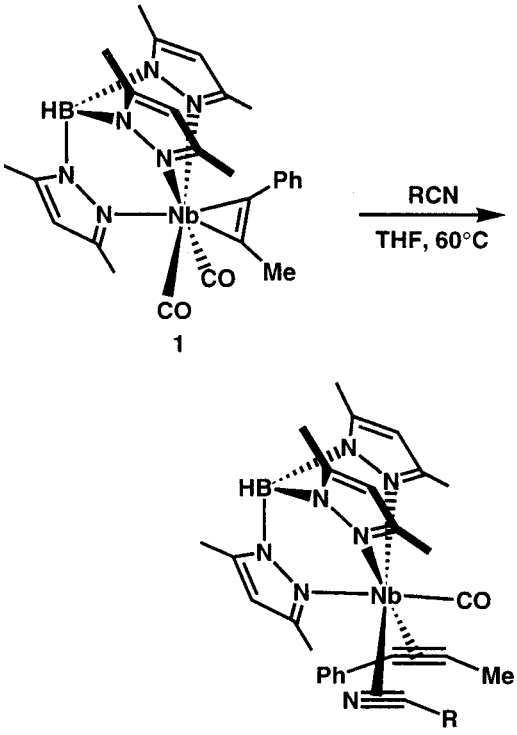

2a (R = Me), 2b (Et), 2c ($PhCH_2$)
2d (4-$MeOC_6H_4$), 2e (Ph), 2f (4-$CF_3C_6H_4$)

The derivatization of transition-metal-bound nitriles has been reviewed.[8] It appears that the vast majority of the reactions involves η^1(2e)-nitrile complexes. Few reactivity studies on η^2(4e)-nitrile complexes have been reported recently.[5,6] In this article we disclose full structural details on unique mixed η^2(3e)-nitrile/η^2(3e)-alkyne complexes bound to (tris(pyrazolyl)borato)niobium(I) centers, some observations concerning their stability and reactivity, as well as comparisons with related bis[(3e)-alkyne] complexes.

Results and Discussion

Synthesis and Spectroscopic Characterization. Treatment of the yellow-green dicarbonyl complex[9] Tp*Nb(CO)$_2$(PhC≡CMe) (**1**; Tp* = hydridotris(3,5-dimethylpyrazolyl)borate) with various nitriles RC≡N in warm thf leads to fair yields of the orange η^2-nitrile adducts Tp*Nb(CO)(PhC≡CMe)(RC≡N) (R = Me (**2a**), Et (**2b**), $PhCH_2$ (**2c**), 4-$MeOC_6H_5$ (**2d**), Ph (**2e**), 4-$CF_3C_6H_5$ (**2f**)) after washing of the crude reaction residue with diethyl ether (Scheme 1). Attempted reactions with malononitrile and fumaronitrile lead to extensive decomposition. The new complexes have been characterized by elemental analyses, IR and NMR spectroscopy, and an X-ray diffraction analysis of **2b**. Key spectroscopic features are collected in Table 1. They are compared with those of related bis(alkyne) derivatives Tp*Nb(CO)(PhC≡CMe)(RC≡CR′) (R = Ph, R′ = Me, **3a**; R = PPh_2, R′ = Ph, **3b**). **3a** has been described previously.[9] Data for the monoalkyne complex **1** and the new phosphine complex **4** are also provided.

A smooth increase of the CO stretch is observed in the IR spectra as the electron-withdrawing ability of the nitrile substituent increases. On the basis of these CO stretching frequencies, phenylpropyne and benzonitrile surprisingly behave similarly. In the solid-state IR spectra, two bands of weak to medium intensity in the 1725−1790 cm^{-1} region are ascribed to ν(CN) and ν(CC) vibrations. Compound **3a** also shows two CC stretches in this region.[9] These low frequencies may be taken as an indication of η^2 coordination. We note, however, that the observation, the wavenumber, nor the intensity of CN stretches has been taken as a fully reliable evidence of either mode of bonding.[1,2,4−6]

The observation of three methine and six methyl resonances in the ^{1}H and ^{13}C NMR spectra testifies to the absence of a symmetry plane in **2a**−**f** (see Experimental Section). These spectra are temperature-independent, especially that of **2b** in thf-d_8 (see below). η^2-Coordination strongly deshields the α-protons of the nitrile. This is clearly seen for the EtCN and $PhCH_2$CN derivatives **2b** and **2c**, respectively. For **2b**, the diastereotopic methylene protons are observed at δ 3.60 and 2.95 as doublets of quartets (^2J = 17, ^3J = 7 Hz).[10] Even more deshielded methylene protons (δ 4.26 and 3.82) have been observed for an η^2(4e)-EtCN complex.[6a] In free propionitrile, the methylene resonance is observed at δ 2.33. For **2c**, the benzylic protons are observed as doublets (^2J = 16 Hz) centered at δ 5.20 and 4.65.

The key spectroscopic technique in solution which allows the definitive assignment of both the hapticity and the formal number of electrons donated by the coordinated nitrile is ^{13}C NMR. However, in the case of compounds **2a**−**f**, the presence of a coordinated phenylpropyne complicates the spectra in the key region. *Three* quarternary carbon resonances are observed in the δ 175−190 region (Table 1). As previously discussed,[3,9] this region is typical of 3e-donor alkyne ligands, and by extension we proposed[7] that a signal in this region could be ascribed to the η^2(3e) behavior of the nitriles. These assignments lead to a formal 18e count for **2a**−**f**. We have conducted two-dimensional ^{1}H−^{13}C HMBC experiments[11] on most of these complexes which now allow us to unambiguously assign the signals either to the nitrile or to the alkyne carbons. The long-range couplings between appropriate protons of the substituent and the contact carbon of the nitrile are relevant. More specifically, for **2c** (see the Supporting Information), coupling between the two benzylic hydrogens with the nitrile carbon at δ 180.1 allows a straightforward definitive assignment. HMBC also differentiates phenyl and methyl attached carbons on the alkyne. A ^3J coupling between the *ortho* phenyl protons yields a single correlation with the carbon resonance at δ 176.6, indicating the phenyl group is attached to this particular niobium-bound carbon. In all cases examined here, the nitrile contact carbon is in the range δ 180−188. It is always deshielded with respect to the coordinated carbons of the (3e)-phenylpropyne. When alkyl nitriles

(8) Michelin, R. A.; Mozzon, M.; Bertani, R. *Coord. Chem. Rev.* **1996**, *147*, 299.
(9) Lorente, P.; Etienne, M.; Donnadieu, B. *An. Quim. Int. Ed.* **1996**, *92*, 88.
(10) In the preliminary communication[7] these chemical shifts were erroneously reported at δ 3.31 and 3.21.
(11) Kusumi, T.; Iwashita, T.; Naoki, H. In *One-dimensional and two-dimensional NMR Spectra by Modern Pulse Techniques*; Nakanishi, K., Ed.; University Science Books: Mill Valley, CA, 1990, and references therein.

Table 1. Key IR and ^{13}C NMR Data for η^2-Nitrile and Alkyne Complexes

complex[a]	ν(CO)[b]	ν(CN)/ν(CC)[c]	δ(*CN*)[d]	δ(*CC*)[d]
[Nb](MeCN) (**2a**)	1913	1785, 1728	180.9	177.3, 174.6
[Nb](EtCN) (**2b**)	1912	1789, 1729	181.9	178.0, 176.6
[Nb]($PhCH_2CN$) (**2c**)	1915		180.1	178.5, 176.6
[Nb]($MeOC_6H_4CN$) (**2d**)	1935		183.1	177.2
[Nb](PhCN) (**2e**)	1940	1737, 1725	186.7	176.6, 176.5
[Nb]($CF_3C_6H_4CN$) (**2f**)	1945		187.9	177.5, 176.6
[Nb](PhCCMe) (**3a**)[e]	1940	1747, 1728		172.1, 165.6
[Nb](Ph_2PCCPh) (**3b**)	1960			190.0, 175.3, 168.9, 167.5
{[Nb]($Ph_2PHCCPh$)}[BF_4] (**3b**-H^+)	2005			216.6, 180.2, 177.6, 139.8
[Nb](CO) (**1**)[e]	1960, 1855			259.4, 212.2
[Nb](PMe_2Ph) (**4**)	1815			216.5, 215.0

[a] [Nb] = Tp*Nb(CO)(PhCCMe). [b] Toluene solution, ±2 cm^{-1}. [c] KBr pellets, ±2 cm^{-1}. [d] Chloroform-*d* (233 K) or benzene-d_6 (room temperature). [e] See ref 9.

Table 2. ^{13}C NMR and X-ray Data for Selected η^2-Nitrile Complexes

complex	*n*[a]	δ(*CN*)	M−C (Å)	M−N (Å)	C−N (Å)	N−C−R (deg)	ref
Cp_2Mo(MeCN)	2	170.8	2.12	2.22	1.21	138	2c,e
$Cp_2Nb(SnMe_3)$(MeCN)	2	179.8, 165.1[b]					2e
$(C_5H_5SiMe_3)_2$NbCl(MeCN)	2	149.4, 144.6[b]					2f
$WCl_2(PMe_3)_3$(MeCN)	4	230	1.97	2.01	1.27	128	4a
$[WCl(bpy)(PMe_3)_2(MeCN)]^+$	4	235	2.00	2.01	1.26	130	4a,b
LWF(CO)(C_6F_5CN)[c]	4	224.1	2.01	2.00	1.26	132	5a
Tp*W(S_2PR_2)(CO)(MeCN)[d]	4	202.1	2.05	2.03	1.23	138	6a
Tp*Nb(CO)(PhCCMe)(EtCN) (**2b**)	3	181.9	2.19	2.16	1.22	140	this work
			2.17[e]	2.12[e]			
Tp*Nb(CO)(PhCCMe)(PhCN) (**2e**)	3	186.7	2.17	2.14	1.21	135	7
			2.17[e]	2.12[e]			

[a] Formal number of electrons donated by the η^2-nitrile. [b] *exo*/*endo* isomers. [c] L = $[C_6H_3CH_2(NMe)(CH_2CH_2NMe_2)]^-$. [d] R = (−)-mentholate. [e] Nb−C bond lengths with the coordinated alkyne, related in a syn manner with Nb−C and Nb−N of coordinated nitrile, respectively (see text).

are considered, the chemical shift difference may be as small as 2 ppm, whereas for the more electron poor nitrile the difference increases to 10 ppm. Considering the shift due to complexation, it is noteworthy that nitrile carbons are less shifted than alkyne carbons here. Free nitrile carbons resonate around δ 120, whereas alkyne carbons appear around δ 80.[12]

In Table 2, we provide spectroscopic and structural comparison for selected η^2(2e)- and η^2(4e)-nitrile complexes. Just as it is the case for alkynes,[3] deshielding of the coordinated nitrile carbon as the formal number of electrons donated to the metal increases is observed. Most η^2(2e)-nitriles exhibit their carbon resonance in the range δ 145−170 with one exception at δ 180. The only η^2(3e)-nitriles reported herein have their carbon resonance in the range δ 180−188. Resonances for η^2-(4e)-nitriles cluster around δ 230, the highest field reported in this case being δ 202.

Electronic spectra of orange aryl nitrile complexes **2d** and **2f** consist of three bands at 436 (sh, ϵ 535), 354 (sh, ϵ 1660), 272 nm (ϵ 15 700 $M^{-1}cm^{-1}$) and 446 (sh, ϵ 310), 362 (sh, ϵ 1180), 262 nm (ϵ 16 120 $M^{-1}cm^{-1}$), respectively. For the propionitrile complex **2b** only a shoulder at 340 nm (ϵ 1950 $M^{-1}cm^{-1}$) accompanies the main absorption at 272 nm (ϵ 9000 $M^{-1}cm^{-1}$). The yellow bis-(alkyne) complex **3a** shows no absorption above the strong UV absorptions at 282 (sh, ϵ 3720) and 250 nm (ϵ 7230 $M^{-1}cm^{-1}$). We ascribe the lower energy band in the 440 nm region for **2d** and **2f** to a d−d band. The high-energy shift as the nitrile becomes more electron-rich is consistent with an increasing HOMO−LUMO gap. The hypsochromic shift is even more pronounced for the bis(alkyne) case. Similar observations and conclusions have been made when comparing η^2(4e)-nitrile and η^2(4e)-alkyne group 6 metal complexes.[4−6]

X-ray Molecular Structure of Tp*Nb(CO)(PhC≡CMe)(EtC≡N) (2b). In our preliminary work,[7] we presented the X-ray molecular structure of the benzonitrile complex **2e**. We felt it of importance to get a new solid-state structure, since the geometric parameters for **2e** were not determined with high accuracy. Also we were struck by the unique arrangement of the ligands and we wondered if an alkyl-substituted nitrile would yield a similar structure. Actually, **2b** and **2e** have very similar overall molecular structures. A view of **2b** is depicted in Figure 1, and selected bond lengths and angles are provided in Table 3. The coordination sphere around the niobium atom can be described as a distorted octahedron if both the phenylpropyne and the propionitrile occupy a single coordination site. The coordinated N(7)−C(3) and C(1)−C(2) bonds are almost perfectly aligned with the Nb(1)−C(4)−O(4) axis. This is a common feature to related bis(alkyne) derivatives[3,9] and η^2(4e)-nitrile complexes,[4−6] and this may be ascribed to optimal orbital interactions. The ethyl group of the nitrile and the methyl group of the alkyne are in a syn relationship with the carbonyl. Exactly the same situation is found for the benzonitrile derivative **2e**. In this respect, we note that the Nb−C and Nb−N bonds with the coordinated alkyne and nitrile are significantly longer for the atoms proximal to the carbonyl (Table 3). This is similarly observed in **2e** (Table 2), in the bis-(phenylpropyne) complex[9] **3a**, and also in the related compound $CpNb(CO)(PhC{\equiv}CPh)_2$.[13] The following bond

(12) Silverstein, R. M.; Bassler, G. C.; Morrill, T. C. *Spectroscopic Identificaton of Organic Compounds*, 4th ed.; Wiley: New York, 1981.

(13) Nesmeyanov, A. N.; Gusev, A. I.; Pasynskii, A. A.; Anisimov, K. N.; Kolobova, N. E.; Struchkov, Yu. T. *J. Chem Soc. D* **1969**, 277.

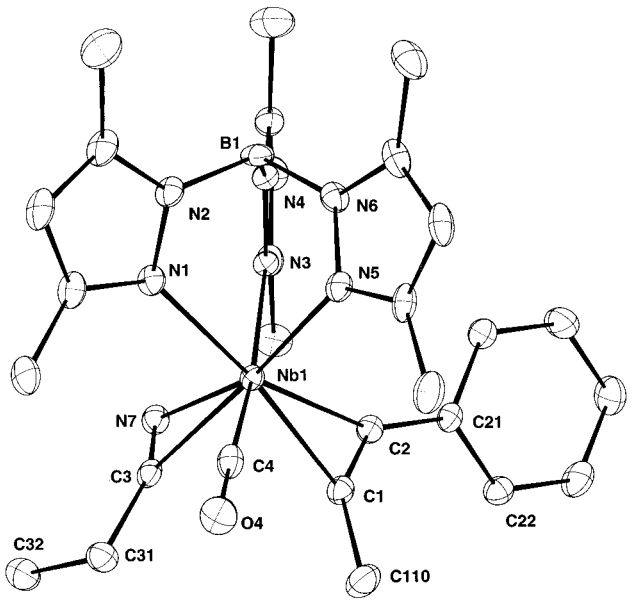

Figure 1. Plot of the molecular structure of Tp*Nb(CO)(EtCN)(PhCCMe) (**2b**).

Table 3. Selected Bond Lengths (Å) and Angles (deg) for Tp*Nb(CO)(PhCCMe)(EtCN) (2b)

Nb(1)−C(1)	2.169(2)	Nb(1)−C(2)	2.121(2)
Nb(1)−C(3)	2.194(2)	Nb(1)−C(4)	2.030(2)
Nb(1)−N(1)	2.318(2)	Nb(1)−N(3)	2.347(2)
Nb(1)−N(5)	2.299(2)	Nb(1)−N(7)	2.159(2)
C(1)−C(2)	1.307(3)	N(7)−C(3)	1.220(3)
O(4)−C(4)	1.169(3)		
Nb(1)−C(1)−C(110)	149.9(2)	Nb(2)−C(2)−C(21)	150.4(2)
Nb(1)−C(1)−C(2)	70.3(1)	Nb(1)−C(2)−C(1)	74.3(1)
Nb(1)−C(3)−C(31)	147.8(2)	Nb(1)−C(3)−N(7)	72.1(1)
Nb(1)−N(7)−C(3)	75.3(1)	N(7)−Nb(1)−C(2)	100.80(7)
N(1)−Nb(1)−C(1)	156.98(8)	N(1)−Nb(1)−C(2)	161.00(7)
N(5)−Nb(1)−C(3)	160.36(8)	N(5)−Nb(1)−N(7)	159.94(7)
C(1)−Nb(1)−C(3)	84.71(8)	Nb(1)−C(4)−O(4)	174.3(2)

lengths are observed within the Nb(EtCN) fragment: Nb(1)−N(7) = 2.159(2), Nb(1)−C(3) = 2.194(2), N(7)−C(3) = 1.220(3) Å. A partial double-bond character between the metal and the nitrile and an elongated CN triple bond are indicated. With reference to the data gathered in Table 2, a monotonic variation of these bonding parameters accompanies the variation in the formal number of electrons *n* donated by the nitrile. Metal−nitrogen bonds can be as short as 2.00 Å for (4e)-nitriles, around 2.15 Å for the (3e)-nitriles reported herein, and finally 2.22 Å for a (2e)-nitrile. Metal−carbon bonds roughly behave in the same way. Elongation of the CN bond when *n* increases testifies to increased $\pi^*_{\|}$ and $\pi_\perp$ interactions. The bend-back angles N−C−R also decrease as *n* increases. Simple electron-counting arguments and the recognition that these complexes are diamagnetic require the presence of a second (3e)-ligand such as phenylpropyne here. Bonding parameters in accord with such a description are observed, with a special mention of very similar Nb−C and Nb−N bonds in the two ligands: Nb(1)−C(1) = 2.169(2), Nb(1)−C(2) = 2.121(2), C(1)−C(2) = 1.307(3) Å. These parameters are comparable to those adopted when two alkynes act as 3e ligands, such as in **3a** (Nb−C = 2.16 Å, average).[9] It is noteworthy that the X-ray-characterized cationic tungsten(II) complex [Tp*W(CO)(PhC≡CPh)(MeC≡N)][BF_4] exhibits (4e)-alkyne and

Table 4. Electrochemical Data for η^2-Nitrile and Alkyne Complexes

complex[a]	E_{red1}	E_{red2}	E_{ox1}	E_{ox2}	E_{ox3}
[Nb](EtCN) (**2b**)[b]	−2.40[c]		−0.15[d]	0.68[e]	1.37[e]
[Nb](MeOC$_6$H$_4$CN) (**2d**)[b]	−2.26[c]		−0.12[d]	0.74[e]	1.36[e]
[Nb](CF$_3$C$_6$H$_4$CN) (**2f**)[b]	−2.13[e]	−1.81[d]		0.95[e]	1.42[e]
[Nb](PhCCMe) (**3a**)	−2.53[c]			0.93[e]	1.30[e]

[a] [Nb] = Tp*Nb(CO)(PhCCMe). [b] Cyclic voltammetry data (E_{red} and E_{ox} are peak potentials for reductive and oxidative processes, respectively, V vs SCE, scan rate 0.1 V s^{-1}) at room temperature in thf with 0.1 M Bu_4NBF_4 as supporting electrolyte and an Au working electrode. [c] Irreversible 2e process. [d] Reversible process, $E = E_{1/2}$. [e] Irreversible 1e process.

η^1(2e)-acetonitrile ligands,[14] despite an identical electron count. In the neutral complex the niobium(I) is a softer center which utilizes the three available π acid ligands.

As previously analyzed for alkynes,[3] it is the absence of a suitable empty metal orbital that leads to the formal 3e-donor behavior. Thus, for symmetry reasons, one electron pair shared by an out-of-phase linear combination of the $\pi_\perp$ orbitals of the alkyne and the nitrile remains nonbonded. This situation leads to an 18e count for these d^4 complexes. Young and co-workers[6a] have carried out extended Hückel calculations on a (4e)-nitrile complex of tungsten. They found that the orbital containing the lone pair on the nitrogen atom mixes with some π-type orbitals upon coordination, leading to a slightly more complex picture. We have carried out similar calculations on the model compounds Tp*Nb(CO)(HC≡CH)(HC≡N) and Tp*Nb(CO)(HC≡CH)$_2$ which confirm this view. However, the calculated net atomic charges are relevant parameters, particularly for rationalizing observed reactivity (see below). Using the atom numbering of Figure 1, N(7) and C(3) bear charges of −0.914 and 0.558 au, respectively, whereas the alkyne carbons C(2) and C(1) bear charges of −0.160 and 0.058 au, respectively. For the bis(alkyne) derivative, charge densities of 0.046 and 0.044 au for the carbons proximal to the carbonyl are computed, whereas the two remote carbons bear −0.196 and −0.213 au. Charges of 0.842 and 0.859 au are computed for the carbonyl carbons of the nitrile alkyne and bis(alkyne) complexes, respectively. Thus, remote atoms of the coordinated alkyne and nitrile with shorter niobium−atom bonds bear more negative charge, and the nitrile is highly polarized.

Reactivity of η^2(3e)-Nitrile and η^2(3e)-Alkyne Complexes. Having highlighted similarities and differences in the structural data for η^2(3e)-nitrile and η^2-(3e)-alkyne complexes, we now describe a comparative reactivity study.

Redox Chemistry. We first address the problem of electron transfers as studied by electrochemical techniques. Representative cyclic voltammetry (CV) data are gathered in Table 4 along with those for the bis(alkyne) complex **3a**. Apart from wave E_{ox1}, the expected positive shift of the potentials for the various processes when the nitrile becomes more electron withdrawing is observed. A splitting of E_{red} into two 1e processes characterizes the reduction of **2f**. The oxidative chemistry is the most interesting. Typical voltammograms for **2b** are depicted in Figure 2. At slow scan rates and at room temperature, three oxidative processes are observed,

(14) Feng, S. G.; Philipp, C. C.; Gamble, A. S.; White, P. S.; Templeton, J. L. *Organometallics* **1991**, *10*, 3504.

Scheme 2. Proposed CE Mechanism for the Oxidation of Tp*Nb(CO)(EtCN)(PhCCMe) (2b)

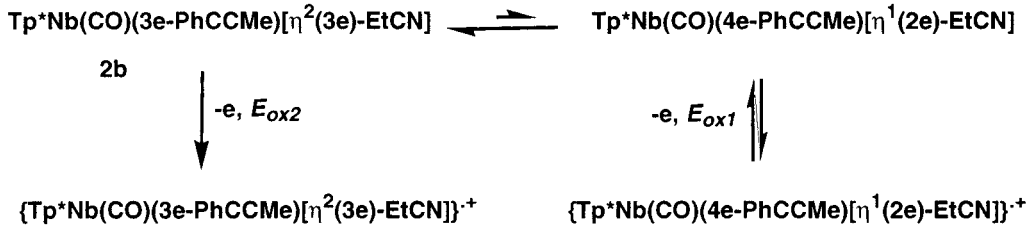

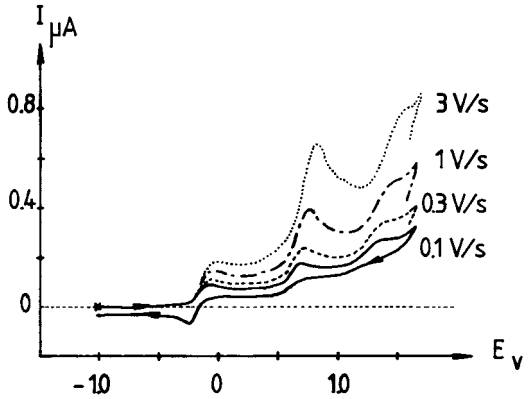

Figure 2. Cyclic voltammograms for Tp*Nb(CO)(EtCN)(PhCCMe) (2b) as a function of scan rate.

with the first one E_{ox1} being reversible. The current function ($i_p^a(ox1)/v^{1/2}$; v = scan rate; i_p^a = anodic peak current) associated with the first oxidation step E_{ox1} decreases with increasing scan rate, indicating that the current is under kinetic control. The ratio of the peak currents of the first two oxidation processes is also dependent on the scan rate ($i_p^a(ox2)/i_p^a(ox1)$ is ca. 1.1 at $v = 0.1$ V s^{-1} and ca. 2.75 at $v = 3$ V s^{-1}; at $v = 100$ V s^{-1} (data not shown), the first process is virtually absent). The ratio also decreases when the temperature is lowered (253 K). These data are all consistent with the electroactive species being produced by a chemical step (CE process).[15] A similar behavior is observed for **2d**. Parallel experiments show that wave E_{ox1}, absent at 0.1 V s^{-1} in the voltammograms of **2f** (Table 4), appears either when the scan rate decreases or when the temperature is increased (313 K). For **2d**, the same behavior is observed whatever the solvent (CH_2Cl_2 or thf), ruling out thf coordination as the process responsible for the CE mechanism. The best chemical description we can think of relies on a preequilibrium process (C part of CE) involving a coupled coordination/electronic change such as an η^2(3e)-/η^1(2e)-nitrile isomerization accompanied by a change in alkyne behavior from (3e)- to (4e)-donor (Scheme 2). Only an undetectable amount (see above the variable-temperature NMR data for **2b** in thf-d_8) of the η^1(2e)-nitrile isomer would be present at room temperature. This isomer would be more easily oxidized than the main η^2(3e) form. Scanning toward positive potentials would shift the equilibrium as the minor isomer is consumed.[16] A time scale of several minutes has been observed for a similar η^2-(2e)/η^1(2e)-nitrile isomerization induced by oxidation of $(C_5H_4SiMe_3)_2NbCl(RC{\equiv}N)$.[2f] No isomerization is involved in the redox behavior of η^2(4e)-nitrile complexes.[4a] Consistent with the proposed CE mechanism, 1 faraday/mol of **2b** is consumed upon electrolysis at the potential of wave E_{ox1}. The primary radical cation **2b**$^{\bullet+}$ is not stable on the electrolysis time scale (as ascertained by CV), although an ESR spectrum characteristic of a niobium-centered radical may be observed ($g = 2.008$). The spectrum is a decet of doublets due to hyperfine couplings with ^{92}Nb ($I = {}^9/_2$, 100% natural abundance, $A_{Nb} = 100$ G) and ^{19}F ($I = {}^1/_2$, 100% natural abundance, $A_F = 23$ G), indicating that tetrafluoroborate from the supporting electrolyte is noninnocent and may transfer a fluoride to an electrophilic species. $Cp_2NbF[CF_3C{=}C(H)CF_3]$ gives a similar ESR spectrum with $g = 1.979$, $A_{Nb} = 111$ G, and $A_F = 28$ G.[17] The fate of this oxidized species has not been studied.

Substitution Chemistry. The substitution chemistry is summarized in Scheme 3. Thermal displacement of the benzonitrile in **2e** is achieved with excess PMe_2Ph. However, reflux in toluene for 3 h is required and considerable decomposition accompanies this reaction. A 35% yield of the green phosphine adduct Tp*Nb(CO)(PMe_2Ph)(PhC≡CMe) (**4**) is obtained. **4** is more conveniently synthesized in 75% yield from dicarbonyl **1** and PMe_2Ph. In **4**, the phenylpropyne behaves as a 4e ligand with contact alkyne carbon resonances observed at δ 216.5 and 215.0. A low-frequency shift of the CO stretch is observed (Table 1). Under similar conditions, no alkyne displacement has been observed in the bis(phenylpropyne) complex **3a**. In warm toluene, phenylpropyne quantitatively displaces benzonitrile in **2e** to give complex **3a**. Similar reactivity patterns have been reported for (4e)-nitrile tungsten(II) complexes.[5,6] The nitrile is thus more labile than the alkyne in these η^2-(3e) complexes.

Protonation Reactions. Owing to the presence of, at least formally, two nonbonding electron pairs in **2a**−**f**, the attack of a proton appeared an efficient way to probe their availablity, from both structural and synthetic viewpoints. Again we have conducted a companion study with the bis(alkyne) complex **3a**. Protonation of the orange benzonitrile complex **2e** at low temperature with tetrafluoroboric acid leads (65% yield) to the dark green azaniobacycle Tp*NbF(CPhCMeCPhNH) (**5**) via a regioselective nitrile/alkyne coupling reaction (Scheme 4). It is noteworthy that the nitrile and alkyne ligands in **2e** are properly set up for the regioselective coupling. **5** has been characterized by analytical and spectroscopic techniques. Evidence for this formulation comes from the IR spectrum of **5**, where N−H and Nb−F stretches are observed at 3382 and 554 cm^{-1}, respec-

(15) Bard, A. J.; Faulkner, L. R. *Electrochemical Methods: Fundamentals and Applications*; Wiley: New York, 1980; Chapter 11, 429−485.

(16) Amatore, C.; Jutand, A.; Khalil, F.; M'Barki, M. A.; Mottier, L. *Organometallics* **1993**, *12*, 3168.

(17) Sala-Pala, J.; Amaudrut, J.; Guerchais, J. E.; Mercier, R.; Douglade, J.; Theobald, J. G. *J. Organomet. Chem.* **1981**, *204*, 347.

Scheme 3

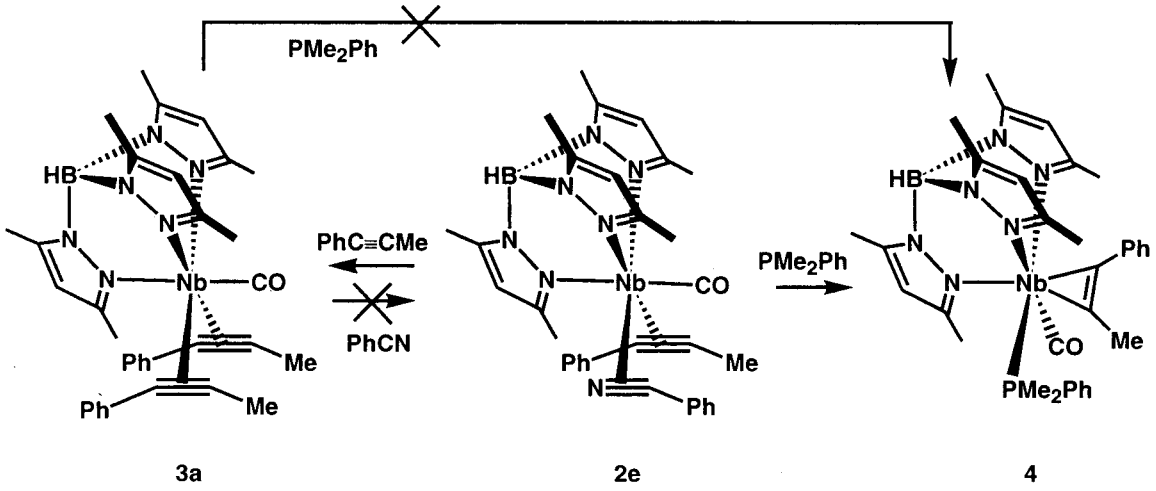

3a 2e 4

Scheme 4

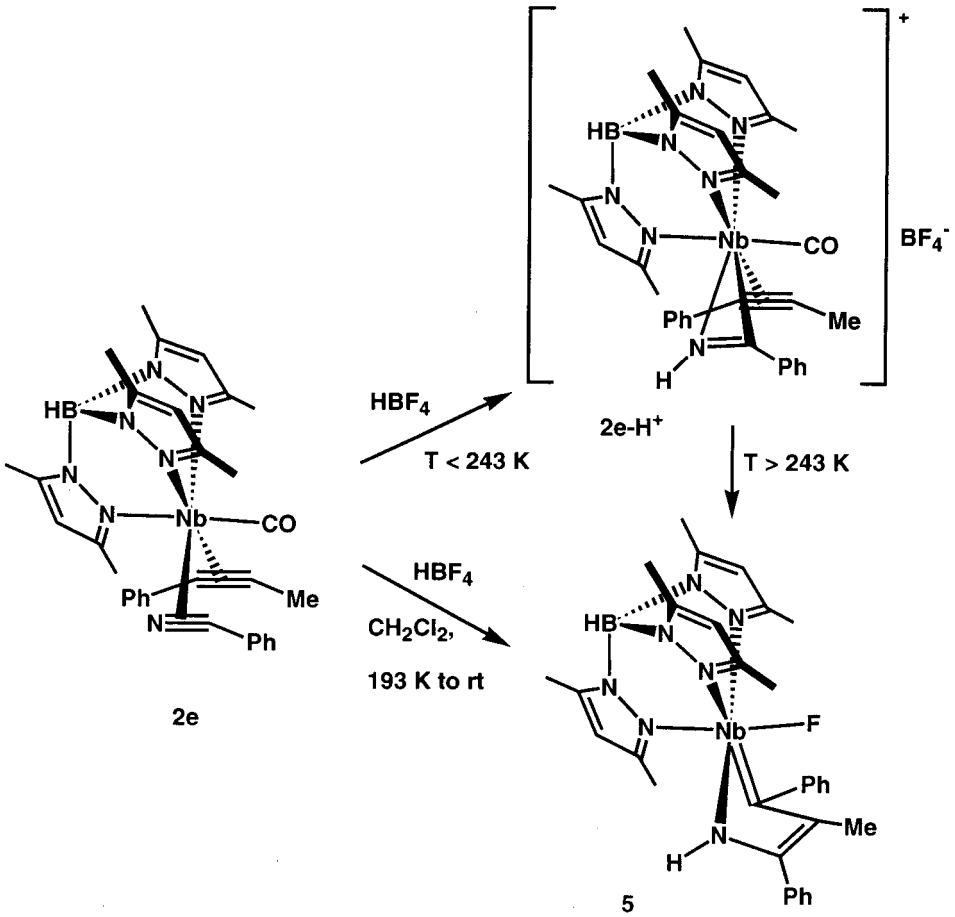

2e 5

tively. The niobium-bound fluoride gives a broad singlet at δ 117 in the ^{19}F NMR spectrum (external trifluoroacetic acid reference). The nitrogen-attached proton gives a slightly broad signal at δ 8.31 in the ^{1}H NMR spectrum, which slowly disappears upon addition of D_2O. ^{13}C NMR signals belonging to quaternary carbons at δ 219.4 (br), 121.8, and 93.6 are ascribed to α-, γ- and β-carbons of the niobacycle, respectively. Similar data have been obtained for related oxa- and azametallacycles of niobium and tantalum,[18] although the secondary nitrogen is unique. These metallacycles are folded along the C_α- - -heteroatom axis, and we assume the same geometry is adopted in **5**. Coupling of nitriles[8] with alkenyl or alkyne ligands at tungsten[19a] and iridium[19b] centers, respectively, has led to related but planar five-membered protonated metallacycles. Similar bent azatitanacycles have recently been obtained through a totally different pathway.[20] We address the mecha-

(18) (a) Curtis, M. D.; Real, J.; Hirpo, W.; Butler, W. M. *Organometallics* **1990**, *9*, 66. (b) Hirpo, W.; Curtis, M. D. *Organometallics* **1994**, *14*, 2706. (c) Etienne, M.; White, P. S.; Templeton, J. L. *Organometallics* **1993**, *12*, 4010.

(19) (a) Legzdins, P.; Lumb, S. A.; Young, V. G. *Organometallics* **1998**, *17*, 854. (b) Alvarado, Y.; Daff, P. J.; Perez, P. J.; Poveda, M. L.; Sanchez-Delgado, R.; Carmona, E. *Organometallics* **1996**, *15*, 2192.

(20) Kahlert, S.; Görls, H.; Scholz, J. *Angew. Chem., Int. Ed.* **1998**, *37*, 1857.

Scheme 5

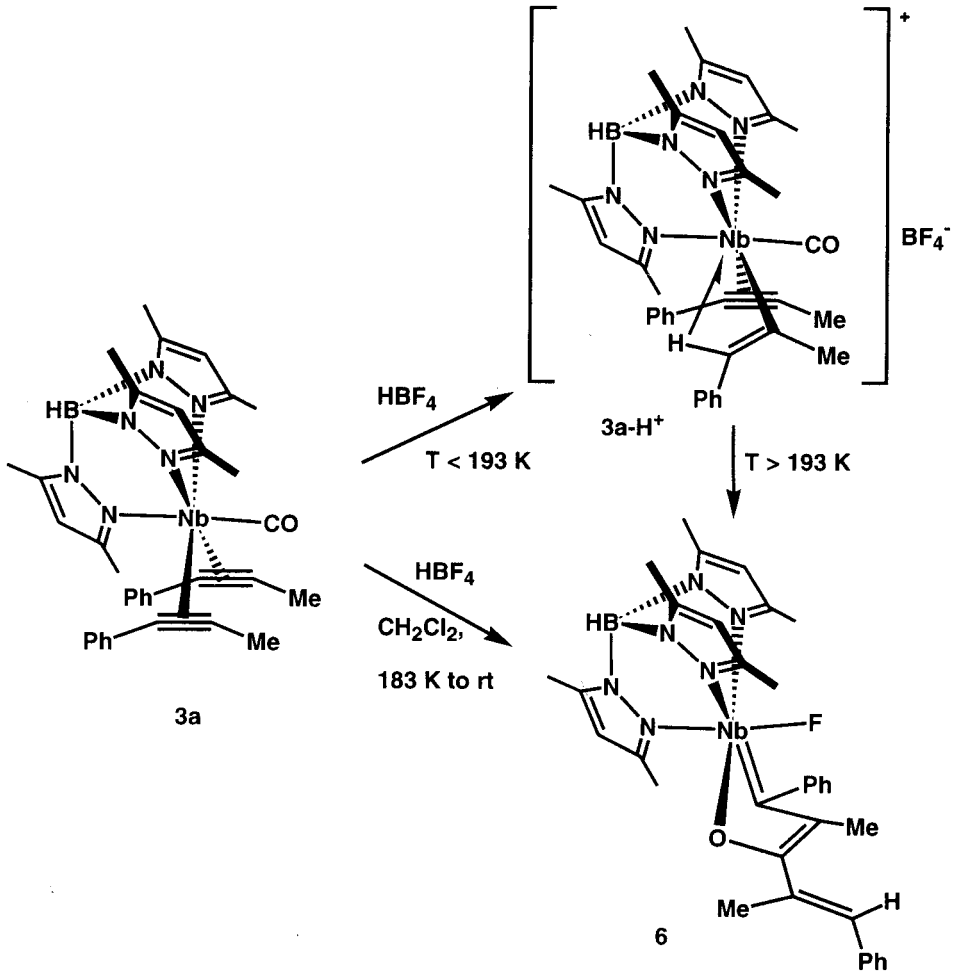

nism by which **5** is formed after presenting the bis(alkyne) behavior.

When the orange bis(phenylpropyne) complex **3a** is similarly protonated at −80 °C, the dark green oxaniobacycle Tp*NbF[C(Ph)C(Me)C(CMe=CPhH)O] (**6**) is isolated in 60% yield (Scheme 5). The IR spectrum again displays no ν(CO) signal but a ν(Nb−F) band at 558 cm^{-1}, and the ^{19}F NMR spectrum gives a Nb−F singlet at δ 122. A ^1H NMR quartet (J = 1.5 Hz) at δ 7.22 integrating for one proton, and the associated methyl doublet at δ 2.44 accounts for the alkenyl group. ^{13}C NMR gives evidence for the α, β, and γ quaternary carbons of the metallacycle at δ 214.9 (br), 102.2, and 141.7 respectively. The exocyclic alkenyl carbons are observed at δ 133.0 (C_δ) and δ 135.3 (C_ϵ, d, J_{CH} = 153 Hz). The regio- and stereochemistry at the *trans*-CMe=CHPh group and the assignment of the carbon skeleton has been ascertained by 2D NMR experiments ($^1H-^1H$ COSY, $^1H-^{13}C$ HMQC, and $^1H-^{13}C$ HMBC) and fully demonstrated after an X-ray diffraction analysis (see below). The retention of the carbonyl group, its insertion into the metallacycle, and the exocyclic alkenyl moiety bearing the delivered proton are noteworthy as compared to the protonation of **2e**. Again the two phenylpropyne ligands in **3a** are perfectly set up for the regioselective coupling. Molybdenum chemistry has produced related couplings. Hydride addition to cationic $[CpMo(CO)(MeC{\equiv}CMe)_2]^+$ in the presence of CO gives the X-ray-characterized neutral planar oxamolybdacycle $CpMo(CO)_2$[C(Me)C(Me)C(CMe=CMeH)O] with an identical stereochemistry at the exocyclic alkenyl group.[21a] Protonation of $CpMoBr(MeCCMe)_2$, where no CO is present, affords a folded metallacycle containing four carbon atoms $\{CpMo(H_2O)(Br)$[C(Me)C(Me)C(Me)=CMeH]$\}^+$.[21b] The recently described isolelectronic tungsten cations $\{Tp^*WCl$[C(Ph)C(Me)C(CH_2Cl)O]$\}^+$ and $\{Tp^*W(NHPh)$[C(Ph)C(Me)C(Me)O]$\}^+$ are similarly bent.[22]

Protonation of the phosphinoalkyne complex **3b** occurs at phosphorus. The resulting phosphonium complex $\{Tp^*Nb(CO)[Ph_2P(H)C{\equiv}CPh](PhC{\equiv}CMe)\}[BF_4]$ (**3b-H$^+$**) is stable as the BF_4^- salt. The hydrogen attached to the phosphorus gives a ^1H NMR doublet at δ 8.55 with a J_{HP} of 516 Hz. According to ^{13}C NMR, a 3e-donor behavior for the two alkynes is appropriate (Table 1). We tentatively assign the doublets at δ 217 (J_{PC} = 22 Hz) and δ 140 (J_{PC} = 45 Hz) to the alkyne carbons attached to the phosphonium and to the phenyl group, respectively. The chemical shifts for the phenylpropyne carbons remain in the normal range. Thus, the filled out-of-phase combination of $\pi_\perp$ alkyne orbitals does not

(21) (a) Allen, S. R.; Green, M.; Norman, N. C.; Paddick, K. E.; Orpen, A. G. *J. Chem. Soc., Dalton Trans.* **1983**, 1625. (b) Fries, A.; Green, M.; Mahon, M. F.; McGrath, T. D.; Nation, C. B. M.; Walker, A. P.; Woolhouse, C. M. *J. Chem. Soc., Dalton Trans.* **1996**, 4517.

(22) (a) Gunnoe, T. B.; Caldarelli, J. L.; White, P. S.; Templeton, J. L. *Angew. Chem., Int. Ed.* **1998**, *37*, 2093. (b) Francisco, L. W.; White, P. S.; Templeton, J. L. *Organometallics* **1997**, *16*, 2547.

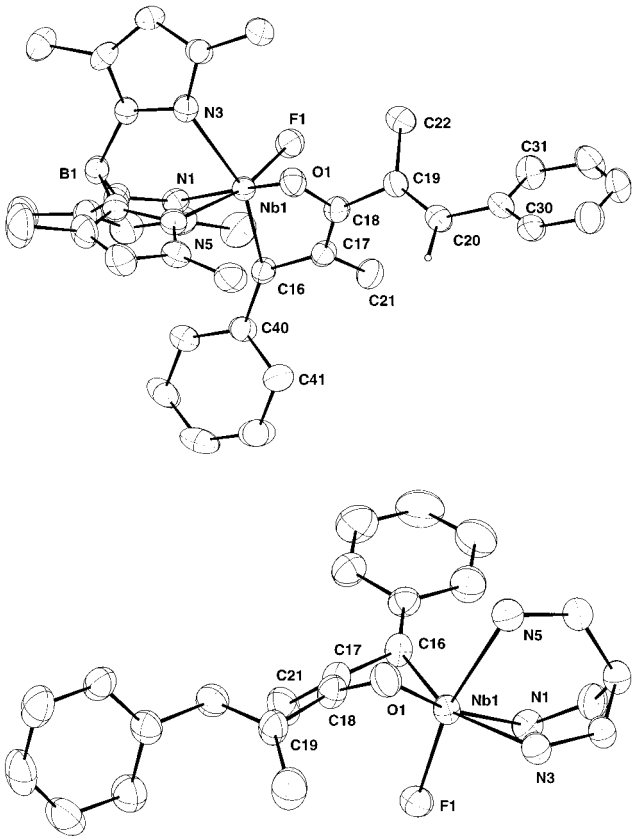

Figure 3. Plots of the molecular structure of Tp*Nb(F)-[C(Ph)C(Me)C(CMe═CPhH)O] **(6)** with *b* emphasizing the folding of the metallacycle (only the nitrogen and boron skeleton of Tp* is shown for clarity).

Table 5. Selected Bond Lengths (Å) and Angles and Torsional Angles (deg) for Tp*NbF[C(Ph)C(Me)C(CMe═CHPh)CO] (6)

Nb(1)−O(1)	1.988(2)	Nb(1)−F(1)	1.925(2)
Nb(1)−C(16)	1.962(4)	Nb(1)−C(17)	2.376(4)
Nb(1)−C(18)	2.387(4)	Nb(1)−N(1)	2.238(4)
Nb(1)−N(3)	2.310(4)	Nb(1)−N(5)	2.277(4)
C(16)−C(17)	1.444(6)	C(17)−C(18)	1.394(6)
C(18)−C(19)	1.492(6)	C(19)−C(20)	1.321(6)
C(18)−O(1)	1.362(5)		

Nb(1)−C(16)−C(17)	87.1(3)	Nb(1)−O(1)−C(18)	88.8(2)
C(16)−C(17)−C(18)	119.1(4)	O(1)−C(18)−C(17)	120.0(4)
C(17)−C(18)−C(19)	123.8(4)	O(1)−C(18)−C(19)	115.7(4)
C(18)−C(19)−C(20)	117.8(4)	C(19)−C(20)−C(30)	128.6(4)
N(1)−Nb(1)−N(3)	78.1(1)	N(1)−Nb(1)−N(5)	83.0(1)
N(3)−Nb(1)−N(5)	76.5(1)	F(1)−Nb(1)−N(1)	90.9(1)
N(1)−Nb(1)−O(1)	169.0(1)	F(1)−Nb(1)−C(16)	111.1(2)
F(1)−Nb(1)−O(1)	99.7(1)		

Nb(1)−C(16)−C(17)−C(18)	39.0
C(17)−C(18)−O(1)−Nb(1)	36.9
O(1)−Nb(1)−C(16)−C(17)	48.2
C(16)−C(17)−C(18)−O(1)	1.2
C(18)−O(1)−Nb(1)−C(16)	49.3

compete with the lone pair on phosphorus for the available proton.

X-ray Molecular Structure of Tp*Nb(F)[C(Ph)C-(Me)C(CMe═CPhH)O] (6). Two different views of **6** are depicted in Figure 3, and selected bond lengths and angles and torsional angles are provided in Table 5. The X-ray analysis confirms the regio- and stereoselectivity of the coupling reaction induced by protonation. The overall coordination, including the folding of the oxaniobacycle along the C(16)- - -O(1) axis, the planarity of the organic part, the alternation of double−single−double−single−double bonds around the metallacyclic ring, and the coordination of the two central carbon atoms, is characteristic of a class of heteroatom-containing metallacyclopentatriene complexes, as analyzed in detail by Curtis and co-workers.[18a,b] Some comparisons are depicted in Chart 1. The group 5 metal complexes all show the same pattern, whereas the oxamolybdacyclopentadiene[21a] is planar with a reversed alternation of single−double bonds. The molybdenum compound and **6** have virtually identical metrical parameters for the exocyclic vinyl group. The Tp*NbF core in **6** leads to slightly shorter Nb−C, Nb−O, and central C−C bonds than Tp*Nb(OMe) in Tp*Nb(OMe)[C(Ph)C(Me)C-(Me)O],[18c] suggesting[18b] slightly enhanced back-donation in the former case. The Nb−F bond length in **6** is comparable to that in $[(C_5H_4Me)_2NbF(CH_2SiMe_3)]^+$ (1.910(2) Å)[23] and shorter than that in $\{[(C_5H_4SiMe_3)_2$-$NbF[\eta^2$-$C(CHPh_2)$═$NPh]\}^+$ (2.199(5) Å).[24]

Chart 1

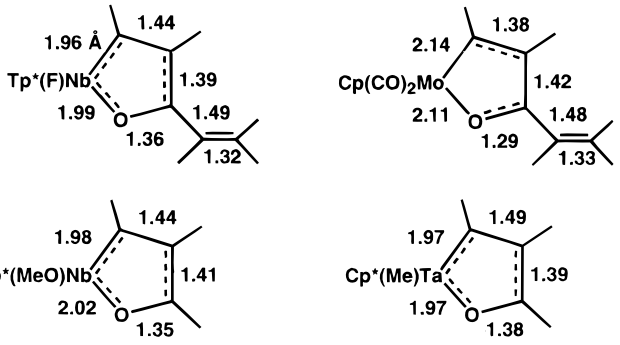

Mechanism of the Protonation of 2e and 3a. Delineating the mechanisms by which transition-metal complexes are protonated still remains a challenge with respect to stereo- and regioselectivity and to thermodynamic versus kinetic control.[25] If we consider the regioselectivity of the protonations of **2e** and **3a**, the orientation of the ligands undergoing the coupling, and the calculated charge densities in the starting compounds, we see that simple proton attack under charge control leads to either secondary iminoacyl alkyne or vinyl alkyne carbonyl cations, respectively. We have conducted low-temperature protonation experiments of **2e** and **3a** directly in NMR tubes in dichloromethane-d_2 in order to observe such putative intermediates.

Protonation of **2e** at 193 K in an NMR tube yields a solution of [Tp*Nb(CO)(η^2-CPh═NH)(PhC≡CMe)][BF_4] (**2e**-**H**$^+$), which can be conveniently observed in situ up to 243 K (Scheme 4). It is also possible to isolate this species: precipitation with ether at 233 K yields a yellow-orange powder which can be washed with cold ether, dried, and redissolved in cold dichloromethane-d_2. However, above 273 K it will convert within minutes to **5**. In the ^{1}H NMR spectrum at 243 K, the ═N*H* proton is observed at δ 13.17 as a slightly broad signal. In the ^{13}C NMR spectrum, four quaternary resonances are observed at δ 218.8, 208.8, 186.7, and 184.9. We ascribe

(23) Fu, P.-F.; Khan, M. A.; Nicholas, K. M. *Organometallics* **1992**, *11*, 2607.
(24) Antinolo, A. Fajardo, M.; Gil-Sanz, R.; Lopez-Mardomingo, C.; Martin-Villa, P.; Otero, A.; Kubicki, M. M.; Mugnier, Y.; El Krami, S.; Mourad, Y. *Organometallics* **1993**, *12*, 381.
(25) Henderson, R. A. *Angew. Chem., Int. Ed. Engl.* **1996**, *35*, 946.

the broad signal at δ 208.8 to Nb*C*O. The two higher field resonances are ascribed to alkyne contact carbons. The most deshielded signal at δ 218.8 belongs to the iminoacyl carbon. We are not aware of any other mononuclear *NH*-iminoacyl complex.[26] Similar data for neutral tantalum iminoacyl alkyne complexes have been obtained.[18a,b] In CpTaMe(η^2-CMe=N^{t}Bu)(ArC≡CAr),[18a] the alkyne and iminoacyl carbons resonate at δ 200 and 241, respectively. Cationic iminoacyl complexes of the type $\{Cp_2NbX[\eta^2\text{-}C(CHRR')=NR'']\}^+$ have the iminoacyl carbon resonance in the δ 215 region.[24] The alkyne carbon chemical shifts indicate competition for the available metal orbitals. Thus, **2e** is first protonated at nitrogen to give an identifiable η^2-*NH*-iminoacyl carbonyl cation **2e**-**H**$^+$, which then loses CO, allowing coupling of the iminoacyl and alkyne moieties.

Protonation of **3a** to give the coupled product **6** is much more rapid. No intermediate is observed above 213 K. Protonation of **3a** at 173 K in an NMR tube in dichloromethane-d_2 yields a solution of [Tp*Nb(CO)(CMe=CPhH)(PhC≡CMe)][BF_4] (**3a**-**H**$^+$), which can be conveniently observed in situ at 193 K (Scheme 5). Definitive assignments of proton and carbon chemical shifts have been obtained through various 2D-NMR techniques (^{1}H−^{1}H COSY, ^{1}H−^{13}C HMQC, and ^{1}H−^{13}C HMBC), so that the regioselectivity of the protonation is ascertained. The vinylic β-H gives a ^{1}H NMR signal at δ 6.91 (br, 1 H). Alkyne carbons give ^{13}C NMR signals at δ 214.8 and 193.7. The vinyl C_α and C_β resonate at δ 204.5 and 97.3, respectively. Shielded C_β appears as a doublet in the ^{1}H-gated spectrum with a reduced $^1J_{CH}$ = 114 Hz indicative of either a pronounced sp^3 character or an elongated C−H bond. These data cannot be fully assigned to either η^1 or η^2-vinyl coordination. The β-H chemical shift is typical of η^1-vinyl ligands.[27] In (η^1-vinyl)niobium complexes, C_α resonances are found in the range δ 165−205,[27a,28] but C_β exhibits clear signs of sp^2 hybridization with a chemical shift around δ 130 and $^1J_{CH}$ in the range 145−165 Hz.[27a,29] Somewhat surprisingly, η^2-vinyl ligands are unknown in group 5 transition-metal complexes,[30] whereas they are common for molybdenum and tungsten. A deshielded C_α (δ 230−290) and a highly shielded C_β (δ 20−30) characterize the η^2 interaction in neutral $CpMo[P(OMe)_3]_2(\eta^2\text{-}CR=CR'R'')$ derivatives.[31] C_β exhibits some vinylic character with a prominent $^1J_{CH}$ of 158 Hz in $W(MA)(S_2CNEt_2)_2\{\eta^2\text{-}CPh=CH[P(OMe)_3]\}$ (MA = maleic anhydride)[32] and $Tp*W(CO)_2(\eta^2\text{-}CPh=CHMe)$.[33] Also, H_β is shielded around δ 3.0−5.0 in these representative complexes.[31−33] Spectroscopic data for rhenium η^2-vinyl cations are similar.[34] Cp*W(NO)(CH_2SiMe_3)(η^2-CPh=CH_2) exhibits a deshielded C_α (δ 228) and chemical shift for C_β (δ 80, $^1J_{CH}$ 146 Hz) between those for η^2-vinyl or η^1-vinyl complexes.[35] The data for **3a**-**H**$^+$ show, however, a very good fit with those of some X-ray-characterized β-agostic[36] vinyl complexes of zirconium. $Cp_2ZrX[C(SiMe_3)=C(\mu\text{-}H)Ph]$ exhibits C_α resonances in the δ 200 region and C_β resonates around δ 110 with a $^1J_{CH}$ of 110−120 Hz.[37] H_β is detected around δ 8.[37] Agostic homo- and heterobimetallic vinylzirconium complexes have produced related spectrocopic data.[38] Thus, such a β-agostic vinyl interaction best fits the data for electrophilic, otherwise unsaturated **3a**-**H**$^+$. The agostic interaction electronically stabilizes **3a**-**H**$^+$ and concomitantly avoids the steric pressure due to an η^2 coordination within the pocket of Tp*.[28] The interplay between steric effects and agostic interactions is a topic of current interest.[39] Also, this interaction provides the proper stereochemistry of the vinyl group. The vinyl cation **3a**-**H**$^+$ is very reactive, and above 213 K, the solution rapidly turns to dark green to give **5**. Here CO is attacked rather than the alkyne. Although there may be some kinetic reasons for that, the formation of a niobium−oxygen bond may also be a thermodynamic driving force for CO incorporation into the metallacycle.

Experimental Section

All experiments were carried out under a dry dinitrogen atmosphere using either Schlenk tube or glovebox techniques. THF and diethyl ether were obtained after refluxing purple solutions of Na/benzophenone under dinitrogen. Toluene, *n*-hexane, pentane, and dichloromethane were dried by refluxing over CaH_2 under dinitrogen. Nitriles were used as soon as possible after reception from the vendor. Deuterated NMR solvents were dried over molecular sieves, degassed by freeze−pump−thaw cycles, and stored under dinitrogen. ^{1}H and ^{13}C NMR spectra were obtained on the following instruments (only pertinent $^1J_{CH}$ values are quoted in the ^{13}C spectra): AM 250, DPX 300, and AMX 400. ^{19}F and ^{31}P NMR spectra were recorded on a Bruker AC 200. Cyclic voltammetry data (homemade potentiostat interfaced with a PC computer): Au working microelectrode (125 μm), THF solution, 0.1 M Bu_4NBF_4 as supporting electrolyte (dried by melting and pumping under vacuum immediately before use), Pt wire as auxiliary electrode, SCE as reference electrode. $Tp*Nb(CO)_2(PhC≡CMe)$ (**1**) and $Tp*Nb(CO)(PhC≡CMe)_2$ (**3a**) were obtained as previously described.[9]

Synthesis of Tp*Nb(CO)(RCN)(PhCCMe) (2a−f). A representative synthesis of **2e** (R = Ph) is as follows. A yellow-green thf solution (20 mL) of complex **1** (0.450 g, 0.80 mmol)

(26) Durfee, L. D.; Rothwell, I. P. *Chem. Rev.* **1988**, *88*, 1059.
(27) (a) Yasuda, H.; Yamamoto, H.; Arai, T.; Nakamura, A.; Chen, J.; Kai, Y.; Kasai, N. *Organometallics* **1991**, *10*, 4058. (b) Herberich, G. E.; Mayer, H. *Organometallics* **1990**, *9*, 2655. (c) Amaudrut, J.; Sala-Pala, J.; Guerchais, J. E.; Mercier, R. *J. Organomet. Chem.* **1990**, *391*, 61.
(28) Etienne, M.; Mathieu, R.; Donnadieu, B. *J. Am. Chem. Soc.* **1997**, *119*, 3218.
(29) Herberich, G. E.; Barlage, W. *Organometallics* **1987**, *6*, 1924.
(30) (a) Labinger, J. A. In *Comprehensive Organometallic Chemistry*; Wilkinson, G., Stone, F. G. A., Abel, E. W., Eds.; Pergamon: New York, 1982; Vol. 3. (b) Wigley, D. E.; Gray, S. D. In *Comprehensive Organometallic Chemistry II*; Abel, E. W., Stone, F. G. A., Wilkinson, G., Eds.; Pergamon: New York, 1995; Vol. 5.
(31) (a) Allen, S. R.; Beevor, R. G.; Green, M.; Norman, N. C.; Orpen, A. G.; Williams, I. D. *J. Chem. Soc., Dalton Trans.* **1985**, 435.
(32) Morrow, J. R.; Tonker, T. L.; Templeton, J. L. *J. Am. Chem. Soc.* **1985**, *107*, 6956.
(33) Feng, S. G.; Templeton, J. L. *Organometallics* **1992**, *11*, 2168.
(34) Casey, C. P.; Brady, J. T.; Boller, T. M.; Weinhold, F.; Hayashi, R. K. *J. Am. Chem. Soc.* **1998**, *120*, 12500.
(35) Debad, J. D.; Legzdins, P.; Lumb, S. A.; Batchelor, R. J.; Einstein, F. W. B. *J. Am. Chem. Soc.* **1995**, *117*, 3288 and Supporting Information therein.
(36) Brookhart, M.; Green, M. L. H.; Wong, L.-L. *Prog. Inorg. Chem.* **1988**, *36*, 1.
(37) Hyla-Kryspin, I.; Gleiter, R.; Kruger, C.; Zwettler, R.; Erker, G. *Organometallics* **1990**, *9*, 517.
(38) (a) Lemke, F. R.; Szalda, D. J.; Bullock, R. M. *J. Am. Chem. Soc.* **1991**, *113*, 8466. (b) Erker, G.; Fromberg, W.; Angermund, K.; Schlund, R.; Kruger, C. *J. Chem. Soc., Chem. Commun.* **1986**, 372.
(39) (a) Jaffart, J.; Mathieu, R.; Etienne, M.; McGrady, J. E.; Eisenstein, O.; Maseras, F. *Chem. Commun.* **1998**, 2011. (b) Haaland, A.; Scherer, W.; Ruud, K.; McGrady, S. G.; Downs, A. J.; Swang, O. *J. Am. Chem. Soc.* **1998**, *120*, 3762. (c) Maseras, F.; Eisenstein, O. *New J. Chem.* **1998**, *22*, 5. (d) Cooper, A. C.; Clot, E.; Huffman, J. C.; Streib, W. E.; Maseras, F.; Eisenstein, O.; Caulton, K. G. *J. Am. Chem. Soc.* **1999**, *121*, 97.

and benzonitrile (0.250 mL, 2.45 mmol) was gently refluxed and monitored periodically by IR spectrocopy. After ca. 90% conversion (ca. 1 h), the dark orange solution was evaporated to dryness. Hexane (20 mL) was added and again stripped off under vacuum to remove traces of thf, leaving an orange to brown solid. The residue was washed with cold ether (0 °C, 3 × 5 mL). Recrystallization from a thf/pentane mixture gave orange microcrystals of **2e**, which were isolated by filtration, washed with pentane (3 × 5 mL), and dried under vacuum (0.330 g, 0.52 mmol, 65% yield).

Tp*Nb(CO)(MeCN)(PhCCMe) (2a). Anal. Calcd for $C_{27}H_{33}BN_7NbO$: C, 56.4; H, 5.8; N, 17.0. Found: C, 56.2; H, 5.6; N, 16.6. Infrared: in toluene, ν(CO) 1913 cm$^{-1;}$ in KBr, ν(CO) 1920, ν(C≡C, C≡N) 1785, 1728 cm^{-1}. ^{1}H NMR (C_6D_6): δ 7.02−6.72 (m, 5 H, C_6H_5), 5.82, 5.37, 5.28 (all s, 1 H, Tp*C*H*), 2.95 (s, 3 H, ≡CCH_3), 2.87 (s, 3 H, CH_3CN), 2.38, 2.19, 2.15, 2.08, 1.98, 1.62 (all s, 3 H, Tp*CH_3). ^{13}C{^{1}H} NMR ($CDCl_3$, 233 K): δ 230.2 (*C*O), 180.9, 177.3, 174.6 (*C*N, Ph*C*≡*C*Me), 153.1, 150.2, 149.6, 144.4, 143.4, 143.3 (Tp**C*CH$_3$), 138.1 (*ipso*-C_6H_5), 128.7 (*m*-C_6H_5), 127.0 (*o*-C_6H_5), 125.8 (*p*-C_6H_5), 107.1, 106.6, 106.1 (Tp**C*H), 17.7, 17.5 (≡C*C*H$_3$ and NC*C*H$_3$), 15.1, 15.0, 14.3, 13.3, 13.2, 13.0 (Tp**C*H$_3$).

Tp*Nb(CO)(EtCN)(PhCCMe) (2b). Anal. Calcd for $C_{28}H_{35}BN_7NbO$: C, 57.1; H, 6.0; N, 16.6. Found: C, 56.2; H, 5.6; N, 16.6. Infrared: in toluene, ν(CO) 1912 cm^{-1}; in KBr, ν(CO) 1894, ν(C≡C, C≡N) 1789, 1729 cm^{-1}. ^{1}H NMR (C_6D_6): δ 6.97 (t, 2 H, J = 7 Hz, *m*-C_6H_5), 6.88 (t, 1 H, J = 7 Hz, *p*-C_6H_5), 6.73 (d, 2 H, J = 7 Hz, *o*-C_6H_5), 5.82, 5.38, 5.28 (all s, 1 H, Tp*C*H*), 3.60 (dq, 1 H, J = 17, 7 Hz, CH_3CH_2CN), 2.98 (s, 3 H, ≡CCH_3), 2.95 (dq, 1 H, J = 17, 7 Hz, CH_3CH_2CN), 2.40, 2.18, 2.16, 2.09, 2.01, 1.62 (all s, 3 H, Tp*CH_3), 1.38 (t, 3 H, J = 7 Hz, CH_3CH$_2$CN). ^{13}C{^{1}H} NMR (C_6D_6): δ 232.8 (*C*O), 181.9 (*C*N), 178.0 (≡*C*Me), 176.6 (≡*C*Ph), 154.6, 153.0, 150.5, 144.2, 143.8, 143.1 (Tp**C*CH$_3$), 139.4 (*ipso*-C_6H_5), 128.5 (*m*-C_6H_5), 127.9 (*o*-C_6H_5), 126.6 (*p*-C_6H_5), 108.1, 107.0, 106.9 (Tp**C*H), 27.0 (CH$_3$*C*H$_2$CN), 18.0 (≡C*C*H$_3$), 15.3, 15.1, 14.9, 13.2, 13.1, 12.9 (Tp**C*H$_3$), 13.9 (*C*H$_3$CH$_2$CN).

Tp*Nb(CO)(PhCH$_2$CN)(PhCCMe) (2c). Anal. Calcd for $C_{33}H_{37}BN_7NbO$: C, 60.85; H, 5.7; N, 15.05. Found: C, 61.10; H, 5.8; N, 14.9. Infrared: in toluene, ν(CO) 1915 cm^{-1}. ^{1}H NMR (C_6D_6): δ 7.55 (d, 2 H, J = 7 Hz, *o*-$C_6H_5CH_2$), 7.27 (t, 2 H, J = 7 Hz, *m*-$C_6H_5CH_2$), 7.15 (t, 1 H, J = 7 Hz, *p*-$C_6H_5CH_2$), 7.09 (t, 2 H, J = 7 Hz, *m*-C_6H_5), 6.97 (t, 1 H, J = 7 Hz, *p*-C_6H_5), 6.81 (d, 2 H, J = 7 Hz, *o*-C_6H_5), 5.95, 5.48, 5.34 (all s, 1 H, Tp*C*H*), 5.20 (d, 1 H, J = 16 Hz, PhCH_2), 4.65 (d, 1 H, J = 16 Hz, PhCH_2), 2.77 (s, 3 H, ≡CCH_3), 2.52, 2.31, 2.27, 2.19, 2.09, 1.70 (all s, 3 H, Tp*CH_3). ^{13}C{^{1}H} NMR (C_6D_6): δ 232.3 (*C*O), 180.1 (*C*N), 178.5 (≡*C*Me), 176.6 (≡*C*Ph), 154.7, 150.5, 144.2, 143.8, 143.1 (Tp**C*CH$_3$), 139.6 (*ipso*-C_6H_5C≡), 136.5 (*ipso*-$C_6H_5CH_2$), 136.5 (*o*-$C_6H_5CH_2$), 128.9 (*m*-$C_6H_5CH_2$), 128.5 (*m*-C_6H_5C≡), 127.9 (*o*-C_6H_5C≡), 127.3 (*p*-$C_6H_5CH_2$), 126.5 (*p*-C_6H_5C≡), 108.2, 107.1, 106.9 (Tp**C*H), 38.5 (Ph*C*H$_2$CN), 17.6 (≡C*C*H$_3$), 15.4, 15.2, 15.1, 13.2, 13.1, 12.9 (Tp**C*H$_3$).

Tp*Nb(CO)(MeOC$_6$H$_4$CN)(PhCCMe) (2d). Anal. Calcd for $C_{33}H_{37}BN_7NbO_2$: C, 59.4; H, 5.6; N, 14.7. Found: C, 59.7; H, 5.9; N, 14.4. Infrared: in toluene, ν(CO) 1935 cm^{-1}. ^{1}H NMR (C_6D_6): δ 8.65 (d, 2 H, J = 9 Hz, *o*-C_6H_4CN), 7.09 (t, 2 H, J = 7 Hz, *m*-C_6H_5), 6.99 (t, 1 H, J = 7 Hz, *p*-C_6H_5), 6.98 (d, 2 H, J = 9 Hz, *o*-C_6H_4OCH$_3$), 6.83 (d, 2 H, J = 7 Hz, *o*-C_6H_5), 6.01, 5.52, 5.33 (all s, 1 H, Tp*C*H*), 3.35 (s, 3 H, ≡CCH_3), 2.53, 2.42, 2.27, 2.18, 2.17, 1.80 (all s, 3 H, Tp*CH_3). ^{13}C{^{1}H} NMR (C_6D_6): δ 183.1 (*C*N), 177.2 (Ph*C*≡*C*Me), 162.2 (*ipso*-C_6H_4OCH$_3$), 154.8, 151.2, 150.1, 144.3, 143.8, 143.1 (Tp**C*CH$_3$), 139.8 (*ipso*-C_6H_5C≡), 133.5 (*o*-C_6H_4CN), 128.2 (*m*-C_6H_5C≡), 127.9 (*o*-C_6H_5C≡), 126.7 (*ipso*-C_6H_4CN), 126.5 (*p*-C_6H_5C≡), 115.0 (*o*-C_6H_4OCH$_3$), 108.3, 107.2, 107.0 (Tp**C*H), 55.0 (O*C*H$_3$), 19.0 (≡C*C*H$_3$), 15.9, 15.7, 15.1, 13.3, 13.1, 12.9 (Tp**C*H$_3$).

Tp*Nb(CO)(PhCN)(PhCCMe) (2e). Anal. Calcd for $C_{32}H_{35}BN_7NbO$: C, 60.3; H, 5.5; N, 15.4. Found: C, 60.3; H, 5.6; N, 15.0. Infrared; in toluene, ν(CO) 1940 cm^{-1}; in KBr, ν(C≡C, C≡N) 1737, 1725 cm^{-1}. ^{1}H NMR (C_6D_6): δ 8.53 (d, 2 H, J = 7 Hz, *o*-C_6H_5CN), 7.29 (t, 2 H, J = 7 Hz, *m*-C_6H_5CN), 7.09 (d, 2 H, J = 7 Hz, *m*-C_6H_5), 6.97 (t, 1 H, J = 7 Hz, *p*-C_6H_5), 6.81 (d, 2 H, J = 7 Hz, *o*-C_6H_5), 5.90, 5.39, 5.19 (all s, 1 H, Tp*C*H*), 3.12 (s, 3 H, ≡CCH_3), 2.40, 2.31, 2.14, 2.06, 1.99, 1.66 (all s, 3 H, Tp*CH_3). ^{13}C{^{1}H} NMR ($CDCl_3$, 243 K): δ 230.1 (*C*O), 186.7 (*C*N), 176.6, 176.5 (Ph*C*≡*C*Me), 153.4, 150.7, 149.8, 144.4, 143.4, 143.2 (Tp**C*CH$_3$), 138.5, 132.3, 130.8, 129.0, 127.7, 127.0, 125.9 (C_6H_5CN and C_6H_5C≡), 107.5, 106.5, 106.3 (Tp**C*H), 18.8 (≡C*C*H$_3$), 15.5, 15.0, 14.7, 13.3, 13.0 (Tp**C*H$_3$).

Tp*Nb(CO)(CF$_3$C$_6$H$_4$CN)(PhCCMe) (2f). Anal. Calcd for $C_{33}H_{34}BF_3N_7NbO$: C, 56.2; H, 4.9; N, 13.9. Found: C, 56.5; H, 5.2; N, 13.7. Infrared: in toluene, ν(CO) 1945 cm^{-1}. ^{1}H NMR: in C_6D_6, δ 8.29, 7.55 (both d, 2 H, J = 8 Hz, $CF_3C_6H_4$-CN), 7.10−6.70 (m, 5 H, J = 7 Hz, *m*-C_6H_5), 5.90, 5.39, 5.21 (all s, 1 H, Tp*C*H*), 3.08 (s, 3 H, ≡CCH_3), 2.39, 2.28, 2.13, 2.05, 1.88, 1.64 (all s, 3 H, Tp*CH_3); in $CDCl_3$ at 243 K, δ 8.39 (d, 2 H, J = 8 Hz, *o*-C_6H_4CN), 7.91 (d, 2 H, J = 7 Hz, *o*-$CF_3C_6H_4$), 7.15 (m, 3 H, *m*- and *p*-C_6H_5), 6.46 (d, 2 H, J = 7 Hz, *o*-C_6H_5), 5.95, 5.66, 5.64 (all s, 1 H, Tp*C*H*), 3.23 (s, 3 H, ≡CCH_3), 2.58, 2.46, 2.34, 1.87, 1.74, 1.69 (all s, 3 H, Tp*CH_3). ^{13}C{^{1}H} NMR ($CDCl_3$, 243 K): δ 229.7 (*C*O), 187.9 (*C*N), 176.6, 177.5 (Ph*C*≡*C*Me), 154.1, 151.2, 150.5, 145.3, 144.2, 144.0 (Tp**C*CH$_3$), 138.8 (*ipso*-C_6H_5C≡), 136.4 (*ipso*-C_6H_4CN), 132.4 (q, J_{CF} = 32 Hz, *ipso*-$CF_3C_6H_4$), 131.4 (*o*-C_6H_4CN), 128.5 (*m*-C_6H_5C≡), 127.7 (*o*-C_6H_5C≡), 126.8 (*o*-$CF_3C_6H_4$), 126.7 (*p*-C_6H_5C≡), 124.4 (q, J_{CF} = 273 Hz, *C*F$_3$), 108.3, 107.3, 107.0 (Tp**C*H), 19.5 (≡C*C*H$_3$), 16.3, 15.7, 15.4, 13.9, 13.7 (Tp**C*H$_3$).

Tp*Nb(CO)(Ph$_2$PCCPh)(PhCCMe) (3b). A yellow-green toluene solution (20 mL) of complex **1** (0.370 g, 0.66 mmol) and Ph_2PCCPh (0.210 g, 0.73 mmol) was gently refluxed for 15 min, during which time it turned yellow-orange. The solution was filtered and concentrated to ca. 3 mL. Addition of pentane (20 mL) yielded an orange powder, which was isolated by filtration, washed with pentane (3 × 5 mL), and dried under vacuum (0.380 g, 0.46 mmol, 70% yield). Anal. Calcd for $C_{45}H_{45}BN_6NbOP$: C, 65.9; H, 5.5; N, 10.2. Found: C, 65.7; H, 5.6; N, 10.0. Infrared: in toluene, ν(CO) 1960 cm^{-1}. ^{1}H NMR (C_6D_6): δ 7.30−6.60 (m, 20 H, C_6H_5), 5.82, 5.54, 5.09 (all s, 1 H, Tp*C*H*), 2.58 (s, 3 H, ≡CCH_3), 2.57, 2.41, 2.38, 2.07, 1.65 (all s, 3 H, Tp*CH_3), 1.40 (d, J_{HP} = 2 Hz, 3 H, Tp*CH_3). ^{13}C{^{1}H} NMR ($CDCl_3$, 243 K): δ 221.3 (*C*O), 190.0 (d, J_{CP} = 8 Hz, Ph_2PC≡), 175.3, 168.9 (Ph*C*≡*C*Me), 167.5 (d, J_{CP} = 53 Hz, Ph_2PC≡*C*Ph), 152.2, 150.2, 150.0, 144.1, 143.4, 142.9 (Tp**C*CH$_3$), 142.8, 140.1, 137.8 (d, J_{CP} = 53 Hz), 135.0 (*ipso*-C_6H_5), 133.5−125.0 (other C_6H_5), 106.9, 106.2, 106.1 (Tp**C*H), 16.9 (≡C*C*H$_3$), 16.6, 16.1, 15.0, 13.3, 13.2 (Tp**C*H$_3$). ^{31}P{^{1}H} NMR ($CDCl_3$): δ 5.4 (*P*PPh$_2$C≡).

{Tp*Nb(CO)[Ph$_2$P(H)CCPh](PhCCMe)}[BF$_4$] (3b-H$^+$). A yellow dichloromethane solution (10 mL) of **3b** (0.155 g, 0.19 mmol) was cooled to −60 °C, and HBF_4·OEt_2 (35 μL, 0.25 mmol) was added via syringe. Slow warming to room temperature was accompanied by a slight color change to reddish. After ca. 45 min, the solution was filtered and the solvent was stripped off. The remaining solid was washed with pentane (3 × 6 mL) and dried under vacuum to give a dark yellow powder (0.155 g, 0.17 mmol, 90%). Anal. Calcd for $C_{45}H_{46}B_2F_4N_6NbOP$: C, 59.5; H, 5.1; N, 9.25. Found: C, 60.2; H, 5.2; N, 9.60. Infrared: in dichloromethane, ν(CO) 2005 cm^{-1}. ^{1}H NMR ($CDCl_3$, 243 K): δ 8.55 (d, J_{HP} = 516 Hz, 1 H, *H*PPh$_2$), 7.50−6.26 (m, 20 H, C_6H_5), 5.95, 5.63, 5.19 (all s, 1 H, Tp*C*H*), 2.75 (s, 3 H, ≡CCH_3), 2.59, 2.42, 2.41, 2.12, 1.60, 1.28 (all s, 3 H, Tp*CH_3). ^{13}C{^{1}H} NMR ($CDCl_3$, 243 K): δ 216.6 (d, J_{CP} = 22 Hz, $Ph_2P(H)C$≡), 216.2 (*C*O), 180.2, 177.6 (Ph*C*≡*C*Me), 152.5, 150.6, 150.0, 145.4, 144.6, 144.1 (Tp**C*CH$_3$), 139.8 (d, J_{CP} = 45 Hz, $Ph_2P(H)C$≡*C*Ph), 137.2 (*ipso*-C_6H_5C≡CMe), 137.1 (d, J_{PC} = 4 Hz, $Ph_2P(H)C$≡C-*ipso*-C_6H_5), 133.5−125.0 (other C_6H_5), 119.3 (d, J_{PC} = 83 Hz, *ipso*-C_6H_5P), 118.7 (d, J_{PC} = 97 Hz, *ipso*-C_6H_5P), 107.9, 107.1, 107.0 (Tp**C*H), 18.0 (≡C*C*H$_3$), 16.2, 15.9, 15.0, 13.6, 13.4, 13.3 (Tp**C*H$_3$). ^{31}P{^{1}H} NMR ($CDCl_3$, 243 K): δ −6.5 (*P*(H)Ph$_2$C≡).

Tp*Nb(CO)(PMe$_2$Ph)(PhCCMe) (4). From Tp*Nb(CO)(PhCN)(PhCCMe) (2e). A toluene solution of **2e** (0.110 g, 0.17 mmol) and PMe$_2$Ph (80 μL, 0.58 mmol) was refluxed in toluene and periodically monitored by IR spectroscopy. The solution slowly turned from yellow-orange to dark brown and became a slurry over the course of ca. 3 h, after which time ν(CO) signals from **2e** were no longer seen. The solution was filtered, evaporated to dryness, and extracted with pentane. The dark green extracts were filtered and evaporated to dryness to yield a dark green solid (ca. 0.040 g, 0.06 mmol, 35%) containing compound **4** ca. 85% pure by ^{1}H NMR.

From Tp*Nb(CO)$_2$(PhCCMe) (1). A toluene solution (30 mL) of **1** (0.400 g, 0.71 mmol) and PMe$_2$Ph (300 μL, 2.1 mmol) was refluxed for ca. 8 h, during which time it turned fom bright yellow-green to dark green. IR monitoring showed complete disappearance of **1**. The solution was evaporated to dryness, and pentane (10 mL) was added and stripped off three times to remove most of the excess phosphine. The solid was redissolved in toluene (20 mL) and the solution filtered through a pad of Celite, which was subsequently washed with toluene (3 × 5 mL). Concentration of this soluton to ca. 3 mL and addition of pentane (20 mL) yielded a green powder which was isolated by filtration, washed with pentane, and dried under vacuum (0.360 g, 0.54 mmol, 75%). Anal. Calcd for $C_{33}H_{41}BN_6NbOP$: C, 58.95; H, 6.15; N, 12.5. Found: C, 58.30; H, 6.30; N, 12.7. Infrared: in toluene, ν(CO) 1815 cm^{-1}. ^{1}H NMR (C_6D_6): δ 7.07−6.75 (m, 10 H, C_6H_5), 5.80, 5.46, 5.45 (all s, 1 H, Tp*C*H*), 3.45 (d, J_{HP} = 1 Hz, 3 H, ≡CCH_3), 2.38, 2.34, 2.25, 2.19, 1.69, 1.40 (all s, 3 H, Tp*CH_3), 1.75, 0.95 (both d, J_{HP} = 6 Hz, 3 H, PCH_3). ^{13}C{^{1}H} NMR (C_6D_6): δ 257.4 (v br, Nb*C*O), 216.5, 215.0 (Ph*C*≡*C*Me), 152.5, 152.3, 148.3, 145.0, 143.9, 143.8 (Tp**C*CH$_3$), 143.2 (*ipso*-C_6H_5C≡), 138.7 (d, J_{PC} = 20 Hz, P−*ipso*-C_6H_5), 131.2 (d, J_{PC} = 14 Hz, P−*m*-C_6H_5), 129.5 (d, J_{PC} = 2 Hz, P−*o*-C_6H_5), 128.3 (P−*p*-C_6H_5), 128.5, 126.9, 125.4 (C_6H_5C≡), 107.0, 106.9, 106.4 (Tp**C*H), 21.3 (≡C*C*H$_3$), 20.4 (d, J_{PC} = 24 Hz, PCH_3), 19.5 (d, J_{PC} = 17 Hz, PCH_3), 16.1 (d, J_{PC} = 3 Hz, Tp**C*H$_3$), 16.0, 15.1, 13.4, 13.2, 13.0 (Tp**C*H$_3$). ^{31}P{^{1}H} NMR (C_6D_6): δ 1.4 (br, $w_{1/2}$ = 110 Hz, Nb*P*).

Tp*Nb(CO)(PhC≡CMe)$_2$ (3a) from Tp*Nb(CO)(PhCN)(PhCCMe) (2e) and PhCCMe. A yellow toluene solution (5 mL) of **2e** (0.070 g, 0.11 mmol) and PhCCMe (130 μL, 1.04 mmol) was warmed at 80 °C with stirring for 2 h. IR and ^{1}H NMR monitoring showed complete conversion of **2e** to **3a**. The volatiles were stripped off under vacuum, and the remaining orange solid was washed with pentane (2 × 3 mL) to give **3a** (0.055 g, 0.08 mmol, 77%), as ascertained by comparison of its ^{1}H NMR spectrum with that of an authentic sample.[9]

Tp*NbF[C(Ph)C(Me)C(Ph)NH] (5). To a cooled (−60 °C) dichloromethane solution (15 mL) of **2e** (0.345 g, 0.54 mmol) was added HBF$_4$·OEt$_2$ (100 μL, 0.68 mmol). A color change from yellow-orange to red occurred upon slow warming to 0 °C. IR monitoring showed no ν(CO). The volatiles were removed under vacuum. The residue was extracted with a toluene/hexane mixture (10 mL of each), and the extracts were filtered through a Celite pad. The solution was stripped to dryness, and recrystallization from toluene/pentane yielded **5** as a red solid (0.220 g, 0.35 mmol, 65%). Anal. Calcd for $C_{31}H_{36}BFN_7Nb$: C, 59.2; H, 5.8; N, 15.6. Found: C, 58.7; H, 5.9; N, 15.3. Infrared: in KBr, ν(Nb−F) 553 cm^{-1}. ^{1}H NMR (C_6D_6): δ 7.92 (d, J = 8 Hz, 2 H, *o*-*Ph*CNH), 7.30 (t, J = 8 Hz, 2 H, *m*-*Ph*CNH), 7.19 (t, J = 8 Hz, 1 H, *p*-*Ph*CNH), 7.04 (d, J = 8 Hz, 2 H, NbC-*m*-*Ph*), 6.90 (d, J = 7 Hz, 2 H, NbC-*o*-*Ph*), 6.69 (t, J = 7 Hz, 1 H, NbC-*p*-*Ph*), 5.39, 5.55, 5.71 (all s, 1 H, Tp*C*H*), 2.38, 2.36, 2.29, 2.24, 2.20, 2.11, 1.30 (all s, 3 H, Tp**Me* and NbCPhC*Me*). ^{13}C{^{1}H} NMR (C_6D_6): δ 219.4 (Nb*C*Ph), 151.6, 151.0, 149.9, 144.4, 143.8, 143.7 (Tp**C*Me), 140.4, 140.0, 130.5, 129.2, 128.6, 128.2, 128.1, 124.3 (NbC*Ph* and NbCPhCMeC*Ph*), 121.7 (NbCPhCMeC*P*h), 106.5, 106.9, 107.1 (Tp**C*H), 93.6 (NbCPh*C*Me), 16.6, 15.7, 14.5 (d, J_{CF} = 5 Hz), 14.3 (d, J_{CF} = 5 Hz), 13.0, 12.7, 12.2 (Tp**Me* and NbCPhC*Me*). ^{19}F{^{1}H} (vs external CF_3CO_2H, C_6D_6): δ 117.1 ($w_{1/2}$ = 30 Hz, Nb*F*).

Tp*NbF[C(Ph)C(Me)C(CMe=CPhH)O] (6). A procedure similar to that used for the synthesis of **5** converted Tp*Nb(CO)(PhC≡CMe)$_2$ (**3a**; 0.360 g, 0.55 mmol) to **6** in the form of green crystals after recrystallization of the crude product from a thf/hexane mixture (0.235 g, 0.35 mmol, 63%). Anal. Calcd for $C_{34}H_{39}BFN_6NbO$: C, 60.9; H, 5.9; N, 12.5. Found: C, 60.6; H, 6.0; N, 12.3. Infrared: in KBr, ν(Nb−F) 558 cm^{-1}. ^{1}H NMR ($CDCl_3$, 263 K): δ 7.55−7.41 (m, 4 H, *p*- and *m*-(C_6H_5)CH=), 7.31 (t, J = 8 Hz, 1 H, *o*-(C_6H_5)CH=), 7.22 (br s, 1 H, =C*H*Ph), 7.05 (d, J = 8 Hz, 2 H, NbC-*m*-*Ph*), 6.79 (t, J = 7 Hz, 1 H, NbC-*p*-*Ph*), 6.37 (d, J = 7 Hz, 2 H, NbC-*o*-*Ph*), 6.02, 5.79, 5.48 (all s, 1 H, Tp*C*H*), 2.47 (s, 3 H, NbC(Ph)C(CH_3)), 2.46 (s, 3 H, C(CH_3)=CHPh), 2.60, 2.42, 2.40, 2.27, 2.08, 1.07 (all s, 3 H, Tp**Me*). ^{13}C{^{1}H} NMR ($CDCl_3$, 263 K): δ 214.9 (Nb*C*Ph), 151.0, 150.8, 149.9, 145.4, 144.2, 143.9 (Tp**C*Me), 141.7 (NbO*C*), 138.3 (NbC(*ipso*-C_6H_5)), 137.3 (CH(*ipso*-C_6H_5)), 135.3 (*C*HPh=), 133.0 (*C*Me=), 129.4 (CH(*o*-C_6H_5)), 128.8 (NbC(*o*-C_6H_5)), 128.3 (CH(*m*-C_6H_5)), 127.5 (NbC(*m*-C_6H_5)), 127.0 (CH(*p*-C_6H_5)), 124.4 (NbC(*p*-C_6H_5)), 107.1, 106.7, 106.4 (Tp**C*H), 102.2 (NbCPh*C*Me), 17.8 (C(*C*H$_3$)=), 17.0 (NbCPhC(*C*H$_3$)), 14.4, 14.3 (d, J_{CF} = 5 Hz), 13.7 (d, J_{CF} = 5 Hz), 13.4, 13.2, 12.5 (Tp**C*H$_3$). ^{19}F{^{1}H} (vs external CF_3CO_2H, $CDCl_3$): δ 122.5 ($w_{1/2}$ = 30 Hz, Nb*F*).

[Tp*Nb(CO)(CPh=NH)(PhCCMe)][BF$_4$] (2e-H$^+$). A cold (−60 °C) yellow dichloromethane solution (10 mL) of **2e** (0.103 g, 0.16 mmol) was treated with HBF$_4$·OEt$_2$ (100 μL, 0.18 mmol). After ca. 15 min, the solution became bright yellow. The solvent was stripped off at −30 °C. The resulting oil was treated with cold (−40 °C) ether to get a yellow powder, which was isolated by filtration, washed with cold (−40 °C) ether, and dried under vacuum at −40 °C. It can be stored several days at this temperature in a freezer before the NMR spectra are run. Alternatively, it has been generated in situ in a cold dichloromethane-d_2 solution (see below the generation of **3a-H$^+$**). ^{1}H NMR (CD_2Cl_2, 243 K): δ 13.17 (s, 1 H, N*H*), 8.44 (d, 2 H, J = 7 Hz, *o*-C_6H_5CN), 7.82 (t, 1 H, J = 7 Hz, *p*-C_6H_5CN), 7.69 (t, 2 H, J = 7 Hz, *m*-C_6H_5CN), 7.20 (d, 1 H, J = 7 Hz, *p*-C_6H_5), 7.15 (t, 2 H, J = 7 Hz, *m*-C_6H_5), 6.39 (d, 2 H, J = 7 Hz, *o*-C_6H_5), 5.96, 5.81, 5.77 (all s, 1 H, Tp*C*H*), 3.37 (s, 3 H, ≡CCH_3), 2.59, 2.46, 2.41, 1.76, 1.67, 1.53 (all s, 3 H, Tp*CH_3). ^{13}C{^{1}H} NMR (CD_2Cl_2, 243 K): δ 218.8 (Nb*C*Ph), 208.8 (br, Nb*C*O), 186.7, 184.9 (Ph*C*≡*C*Me), 153.4, 151.2, 150.7, 146.4, 145.7, 145.3 (Tp**C*CH$_3$), 135.6, 134.8, 131.5, 130.0, 129.0, 128.1, 128.0, 127.4 (C_6H_5CN and C_6H_5C≡), 107.7, 107.4, 107.3 (Tp**C*H), 20.9 (≡C*C*H$_3$), 15.4, 14.6, 13.7, 13.0, 12.9, 12.5 (Tp**C*H$_3$).

[Tp*Nb(CO)(CMe=CPhH)(PhCCMe)][BF$_4$] (3a-H$^+$). Tp*Nb(CO)(PhC≡CMe)$_2$ (**3a**; 0.039 g, 0. 06 mmol) was dissolved in dichloromethane-d_2 (0.5 mL) in a 5 mm NMR tube fitted with a rubber septum. The tube was cooled to 173 K in an ethanol−liquid dinitrogen slush bath. The yellow-orange solution was treated with HBF$_4$·OEt$_2$ (50 μL, 0.09 mmol) added via syringe through the septum. The tube was shaken at this temperature to give a bright orange solution upon mixing. The tube was then introduced in the precooled (193 K) probe of the AMX 400 spectrometer for analyses. ^{1}H NMR (CD_2Cl_2, 193 K): δ 7.35 (m, C_6H_5), 7.18 (m, C_6H_5), 6.93 (m, C_6H_5), 6.91 (br, 1 H, NbCMe=C*H*Ph), 6.30 (br, C_6H_5), 6.25 (br, C_6H_5), 6.02, 5.95, 5.76 (all s, 1 H, Tp*C*H*), 3.63 (s, 3 H, ≡CCH_3), 3.42 (s, 3 H, NbCCH_3=CHPh), 2.62, 2.45, 2.43, 1.94, 1.57, 1.04 (all s, 3 H, Tp*CH_3). ^{13}C NMR (CD_2Cl_2, 193 K): δ 214.8 (PhC≡*C*Me), 204.5 (Nb*C*Me), 203.1 (br, Nb*C*O), 193.7 (Ph*C*≡CMe), 154.3, 152.2, 151.4, 147.0, 146.9, 146.4 (Tp**C*CH$_3$), 134.2, 130.1 (*ipso*-*Ph*), 128.9, 28.7 128.1, 127.5, 127.1, 126.5 (CHC_6H_5 and C_6H_5C≡), 108.4, 107.9, 107.5 (Tp**C*H*), 97.3 (d, J = 114 Hz, =*C*HPh), 22.7 (q, J = 130 Hz, NbC*C*H$_3$), 21.3 (≡C*C*H$_3$), 15.2, 14.9, 13.8, 13.4, 13.0, 12.7 (Tp**C*H$_3$).

Table 6. Crystal Data, Data Collection and Refinement Parameters for the X-ray Diffraction Analysis of Compounds 2b and 6

	2b	**6**
	Crystal Data	
chem formula	$C_{26}H_{33}BN_7NbO\cdot 1.5C_6H_6$	$C_{34}H_{39}BFN_6NbO$
cryst syst	triclinic	monoclinic
space group	$P\bar{1}$	$P2_1/c$
a (Å)	11.738(2)	13.314(4)
b (Å)	12.607(2)	16.800(4)
c (Å)	13.073(2)	16.101(5)
α (deg)	67.03(2)	90.0
β (deg)	85.25(2)	111.79(3)
γ (deg)	80.31(2)	90.0
V (Å^3)	1755(1)	3344(2)
Z	2	4
μ (cm^{-1})	0.37	0.38
	Data Collection	
diffractometer	STOE IPDS	STOE IPDS
radiation type	Mo Kα	Mo Kα
wavelength (Å)	0.710 73 (graphite monochr)	0.710 73 (graphite monochr)
temp (K)	160	293
2θ range (deg)	3.5−48.5	3.6−48.1
hkl range	$-13 \le h \le 13$ $-12 \le k \le 14$ $0 \le l \le 14$	$-15 \le h \le 14$ $0 \le k \le 18$ $0 \le l \le 18$
no. of measd rflns	10 226	20 785
no. of indep rflns	5219	5201
merging R value	0.0246	0.051
	Refinement	
refinement on	F	F
R^a	0.0261	0.0390
$R_w{}^b$	0.0322	0.0279
GOF (S)^c	1.155	1.10
weighting scheme	Chebychev^d	Chebychev^d
coeffs Ar^d	1.39, −0.0294, 1.11	0.245, −1.57, 0.246, −0.672
no. of rflns used	4225 ($I > 3\sigma(I)$)	3137 ($I > 2\sigma(I)$)
no. of params used	416	400

^{a} $R = \sum(||F_o| - |F_c||)/\sum|F_o|$. ^{b} $R_w = [\sum w(||F_o| - |F_c||)^2/\sum(|F_o|)^2]^{1/2}$. ^{c} Goodness of fit $= [\sum(|F_o - F_c|)^2/(N_{observns} - N_{params})]^{1/2}$. ^{d} $w = w'[1 - (\Delta F/6\sigma(F))^2]^2$. $w' = 1/\sum(r = 1,3)\ \mathrm{Ar}\mathrm{Tr}(x)$, where Ar are the coefficients for the Chebyshev polynomial $\mathrm{Tr}(x)$ with $x = F_c/F_c(\max)$.

Crystallographic Studies. Single crystals of **2b** were obtained from a benzene-d_6 solution. Those of **6** were grown from a thf/hexane solution. A summary of experimental and refinement data is presented in Table 6. The data collection (for **2a**, $T = 160$ K; for **6**, $T = 293$ K) was performed on a STOE IPDS diffractometer using graphite-monochromated Mo Kα radiation. The structure was solved by direct methods using SIR92[40] and subsequent difference Fourier maps. No absorption corrections were made. The refinement was carried out with the CRYSTALS package.[41] All atoms, except hydrogens, were anisotropically refined, including those of the solvent (1.5 C_6H_6 molecule in the asymmetric unit for **2b**). Except for H(1) bound to B(1) in **6**, which was observed in a difference Fourier map and subsequently refined with an fixed isotropic thermal parameter, all hydrogen atoms were included in the calculation in idealized positions (C−H = B−H = 0.96 Å) with an isotropic thermal parameter 1.2 times that of the atom to which they were attached. Full-matrix least-squares refinements were carried out by minimizing the function $\sum w(||F_o| - ||F_c|)^2$, where F_o and F_c are the observed and calculated structure factors. A weighting scheme was introduced with $w = w'[1 - (\Delta F/6\sigma(F))^2]^2$.[42] The model reached convergence with $R = \sum(||F_o| - ||F_c|)/\sum|F_o|$ and $R_w = [\sum w(||F_o| - |F_c||)^2/\sum w(|F_o|)^2]^{1/2}$ having values listed in Table 6. Plots of molecular structures (for **2b**, Figure 1; for **6**, Figure 3) were obtained by using the software CAMERON.[43]

Acknowledgment. Bruno Donnadieu (acquisition of X-ray data) and Francis Lacassin and Gilles Pelletier (high-field NMR) are thanked for their skillful assistance. Helpful discussions about the electrochemical studies with Drs A. Jutand (ENS-CNRS, Paris) and J. Talarmin (UBO-CNRS, Brest) are acknowledeged. C.C. and M.E. thank the Commission of the European Communities and the LCC for an HCM grant to C.C. under Contract No. ERBCHBGCT930417.

Supporting Information Available: A figure giving an expanded region of the $^1H-^{13}C$ HMBC NMR spectrum of **2c** and tables providing full structural details, fractional atomic coordinates, anisotropic thermal parameters, and bond lengths and angles for compounds **2b** and **6**. This material is available free of charge via the Internet at http://pubs.acs.org.

OM990119K

(40) Altomare, A.; Cascarano, G.; Giacovazzo, G.; Guargliardi, A.; Burla, M. C.; Polidori, G.; Camalli, M. SIR 92, a Program for Automatic Solution of Crystal Structures by Direct Methods. *J. Appl. Crystallogr.* **1994**, *27*, 435.

(41) Watkin, D. J.; Prout, C. K.; Carruthers, R. J.; Betteridge, P. CRYSTALS Issue 10; University of Oxford, Oxford, U.K., 1996.

(42) Carruthers, J. R.; Watkin, D. J. *Acta Crystallogr.* **1979**, *A35*, 698.

(43) Watkin, D. J.; Prout, C. K.; Pearce, L. J. CAMERON; University of Oxford, Oxford, U.K., 1996.